Shock and Vibration 19 (2012) 57–79
DOI 10.3233/SAV-2012-0616
IOS Press

An efficient approach for determining forced vibration response amplitudes of a MDOF system with various attachments

J.S. Wu* and J.H. Chen
Department of Systems and Naval Mechatronic Engineering, National Cheng-Kung University, Tainan, Taiwan

Received 25 June 2009
Revised 17 April 2010

Abstract. The frequency-response curve is an important information for the structural design, but the conventional time-history method for obtaining the frequency-response curve of a multi-degree-of-freedom (MDOF) system is time-consuming. Thus, this paper presents an efficient technique to determine the forced vibration response amplitudes of a multi-span beam carrying arbitrary concentrated elements. To this end, the "steady" response amplitudes $|Y(x)|_s$ of the above-mentioned MDOF system due to harmonic excitations (with the specified frequencies ω_e) are determined by using the numerical assembly method (NAM). Next, the corresponding "total" response amplitudes $|Y(x)|_t$ of the same vibrating system are calculated by using a relationship between $|Y(x)|_t$ and $|Y(x)|_s$ obtained from the single-degree-of-freedom (SDOF) vibrating system. It is noted that, near resonance (i.e., $\omega_e/\omega \approx 1.0$), the entire MDOF system (with natural frequency ω) will vibrate synchronously in a certain mode and can be modeled by a SDOF system. Finally, the conventional finite element method (FEM) incorporated with the Newmark's direct integration method is also used to determine the "total" response amplitudes $|Y(x)|_t$ of the same forced vibrating system from the time histories of dynamic responses at each specified exciting frequency ω_e. It has been found that the numerical results of the presented approach are in good agreement with those of FEM, this confirms the reliability of the presented theory. Because the CPU time required by the presented approach is less than 1% of that required by the conventional FEM, the presented approach should be an efficient technique for the title problem.

Keywords: Frequency-response curve, steady response amplitude, total response amplitude, numerical assembly method, finite element method

1. Introduction

Because the mathematical model of some vibrating systems can be established by using a uniform or non-uniform beam carrying various concentrated elements (such as lumped masses with rotary inertias, linear springs and/or rotational springs) with various boundary (supporting) conditions, the literature concerned is plenty [1–22]. Among the above-mentioned references, most of them concerning the "free" vibration analysis [1–17] and those relating to the "forced" vibration analysis is relatively fewer [18–22]. For the "free" vibration analysis of beams with various attachments (such as rigidly or elastically attached point masses, translational or rotational springs), some classical analytical methods were presented [1–8]. Since the last analytical methods suffer difficulty when the total number of attachments on the beam is great than two, an approximate analytical-and-numerical- combined method (ANCM) was presented [9,10]. In recent years, some researchers obtained the "exact" solutions for free vibration of a complicated beam carrying any number of concentrated elements with various supporting conditions by using the numerical

*Corresponding author. E-mail: jswu@mail.ncku.edu.tw.

ISSN 1070-9622/12/$27.50 © 2012 – IOS Press and the authors. All rights reserved

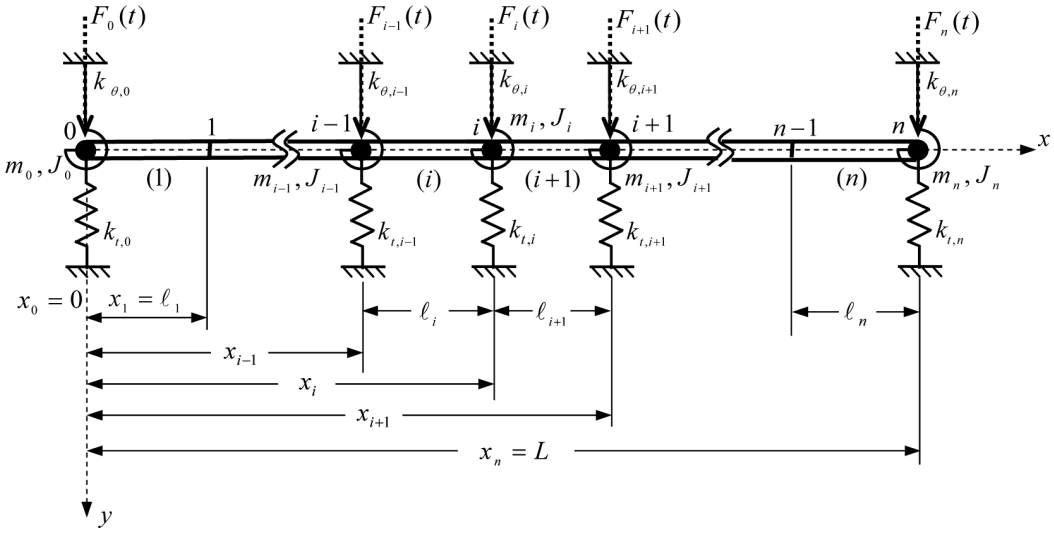

Fig. 1. A uniform *free-free* beam composed of n uniform beam segments (denoted by (1), (2), . . . , (i-1), (i), (i+ 1), . . . , (n)) separated by $n-$ 1 nodes (denoted by 1, 2, . . . , $i-$ 1, i, $i+$ 1, . . . , $n-$ 1) and carrying a lumped mass $\hat{m}_i$ (with rotary inertia J_i), a translational spring k_{ti}, a rotational spring $k_{\theta i}$ and a concentrated force $F_i(t)$ at each node i, $i = 0,1,2, \ldots, n$.

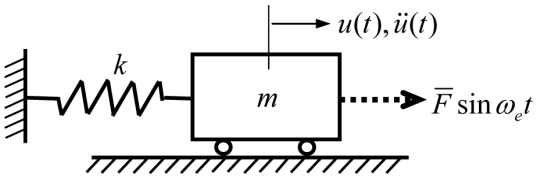

Fig. 2. A SDOF spring-mass system subjected to a harmonic force $\bar{F}\sin\omega_e t$.

assembly method (NAM) [11–13], and the "approximate" solutions for free vibration of rotor-bearing systems by using the transfer matrix method (TMM) [14–17]. For the "forced" vibration problem of beams with various attachments, it is solved with the polynomial coordinate function method [18], mode superposition method [19,20], Green function method [21] or numerical assembly method [22].

From the foregoing literature review one finds that, for the free vibration analyses of various beams (such as uniform beam, stepped beam, tapered beam, etc.) carrying any number of various concentrated elements (such as linear spring, rotational spring, lumped mass with rotary inertia and eccentricity) with various boundary conditions (such as free-free, clamped-clamped, pinned-pinned, clamped-free, clamped-pinned or intermediate supports), the NAM is one of the effective approaches. However, the information regarding NAM to be applied to the forced vibration analysis of structural systems is little and reference [22] is found to be the one most concerned. In reference [22], based on the formulation of NAM [11–13], Lin obtained a matrix equation of the form $[B]\{C\} = \{\bar{F}\}$ by considering the effect of a harmonic exciting force $F_i(t)$ with the specified exciting frequency ω_e, the compatibilities of deformations and the equilibriums of forces (including moments) at the attaching points of the concentrated elements and at the two ends of the beam. In the last equation, $[B]$ is a coefficient matrix to be a function of ω_e, $\{C\}$is a column vector of unknown integration constants of all beam segments composed of the entire beam and $\{\bar{F}\}$ is a column vector consisting of the exciting force amplitudes $\bar{F}_i$. It is evident that from the relation $\{C\} = [B]^{-1}\{\bar{F}\}$ one can obtain the integration constant vector $\{C\}$ and, in turn, the corresponding vibration response amplitude curve. However, from the formulation of reference [22], one finds that the last vibration response amplitude is only the "steady" component $|Y(x)|_s$ (associated with the exciting frequency ω_e) of the "total" response amplitude $|Y(x)|_t$ and the "complementary" component $|Y(x)|_c$ (associated with the natural frequency ω of the vibrating system) is not considered. For this reason, the vibration response amplitude $|Y(x)|_s$ obtained from reference [22] is much smaller than that ($|Y(x)|_t$) obtained from the conventional finite element method (FEM) [23,24]. In this paper, a

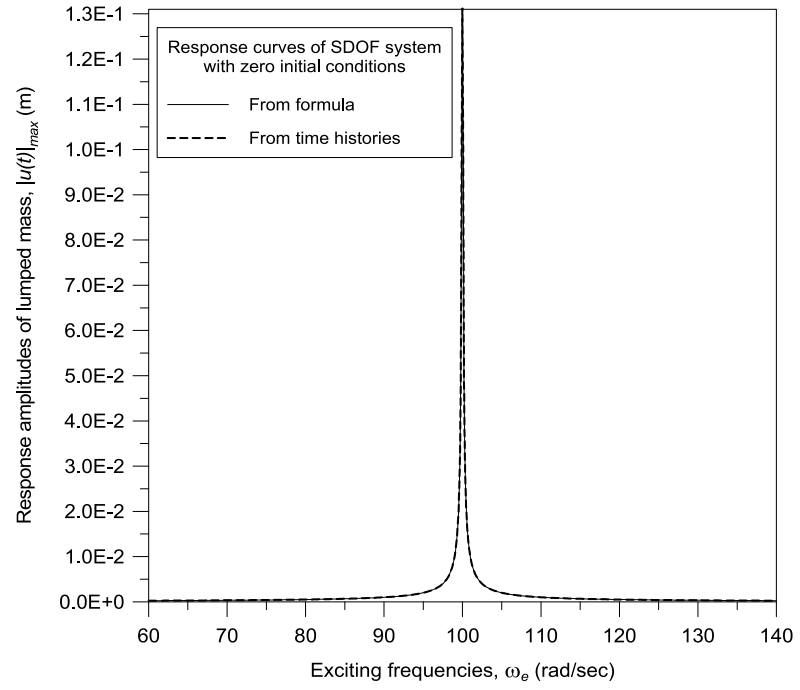

(a)

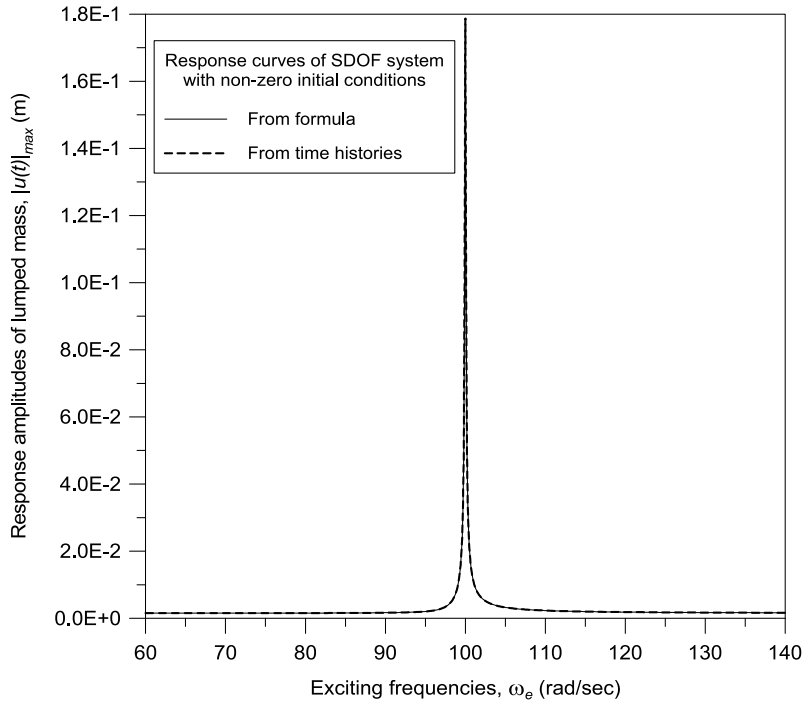

(b)

Fig. 3. The frequency-response curves for the total amplitudes obtained from formula $\bar{u}_t = |\bar{u}_s| + |\bar{u}_c|$ (or $\bar{u}_t = |\bar{u}_s| + \bar{U}_c$) (denoted by —) and conventional time histories $\bar{u}_t = |u(t)|_{\max}$ (denoted by $- - -$): (a) with "zero" initial conditions (i.e., $u_0 = \dot{u}_0 = 0$); (b) with "non-zero" initial conditions (i.e., $u_0 = 0.001$ m and $\dot{u}_0 = 0.1$ m/sec).

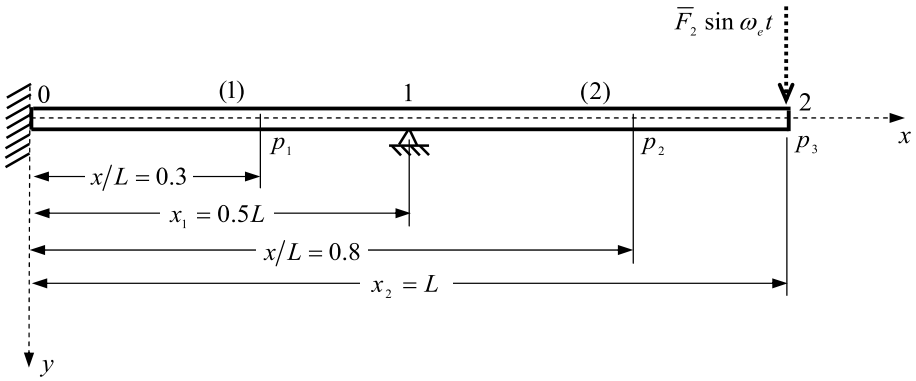

Fig. 4. A cantilever beam with an intermediate pinned support at mid-length (node 1) and subjected to a harmonic concentrated force $\bar{F}_2 \sin \omega_e t$ at free end (node 2).

simple approach is presented to determine the total response amplitude of a vibrating system by using NAM [22] and the relationship $|Y(x)|_t = [1 + (\omega_e/\omega)] \cdot |Y(x)|_s$. The last relationship is derived from a single-degree-of- freedom (SDOF) system and can also be extended to the multi-degree-of-freedom (MDOF) system, since, near resonance (with $\omega_e/\omega \approx 1.0$), the entire MDOF system will vibrate synchronously in a certain mode (looking like a SDOF system) and can be modeled by a SDOF system as one may see from reference [23] and the numerical examples presented in this paper. The frequency-response amplitude curves denoted by the solid lines (—) shown in Figs 5, 7–10 of this paper are obtained from the above-mentioned approach.

In order to confirm the reliability of the presented approach, the complete solution for the forced (transient) vibration responses of the multi-span beam carrying various concentrated elements and subjected to external harmonic excitations (as shown in Fig. 6) is also determined by using the conventional FEM and the step-by-step numerical integration method [24], and, corresponding to each specified exciting frequency ω_e, the "total" vibration response amplitude for each point of the beam is obtained from the maximum absolute response $|y(x,t)|_{\max}$ of its time history of transverse displacements, $y(x,t)$. Since the frequency-response amplitude curves denoted by the dashed lines (- - - - -) shown in Figs 5, 7–10 of this paper are obtained from this conventional FEM, good agreement between the solid curves (based on the presented approach) and the corresponding dashed curves (based on the conventional FEM) may be the fact that the presented approach is reliable.

The formulation of this paper is based on the "continuous" model and that of the conventional FEM is based on the "discrete" model. One of the main differences between the "continuous" model and the "discrete" model is that the degree of freedom (DOF) of the former is *infinite* and that of the latter is *finite*. Thus, the results based on the "continuous" model are the "exact" solutions and those based on the "discrete" model are the "approximate" solutions [25]. This is one of the merits for the presented approach to be better than the conventional FEM. Furthermore, because the formulation of this manuscript is based on the "continuous" model, for the uniform beam shown in Fig. 1 carrying s sets of "intermediate concentrated elements" (ICE's) with each set of ICE's consisting of a linear spring k_{ti}, a rotational spring $k_{\theta i}$ and a lumped mass $\hat{m}_i$ (with rotary inertia J_i), one can model the entire beam by using only $s + 1$ beam segments to achieve the "exact" solutions. In other words, for a uniform beam carrying 5 ICE's, one requires a mathematical model consisting of only 6 beam segments (such as that shown in Fig. 6) to arrive at the exact solutions. However, this is not true for the FEM, because the accuracy of its numerical results are significantly dependent on the total number of beam elements ($n_e = 80$ for the beam shown in Fig. 6). This is the reason why the input data required by the developed computer program based on the formulation of NAM is simpler than those required by the conventional FEM, as a result, the storage memory and computing time required by NAM are much smaller than those required by FEM.

2. Determination of "steady" response amplitudes by using NAM

This section presents the theory of determining the "steady" response amplitudes of a uniform multi-span beam carrying various concentrated elements (cf. Fig. 1) by using the numerical assembly method (NAM) [11,22].

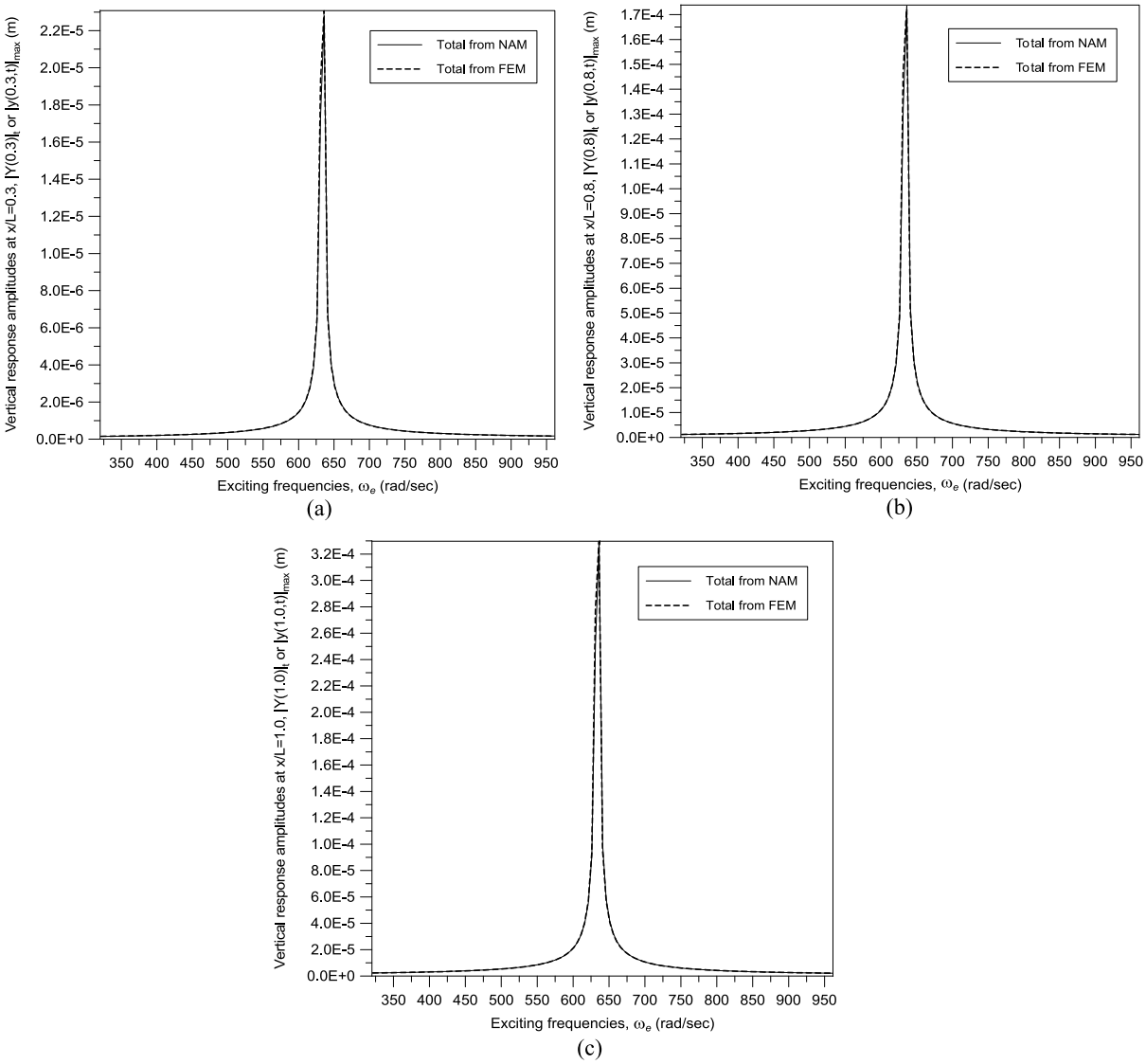

Fig. 5. The frequency-response curves for the three points p_1, p_2 and p_3 on the beam (with "zero" initial conditions) shown in Fig. 4 located at: (a)$\xi = x/L$ =0.3, (b)$\xi = x/L$ =0.8 and (c)$\xi = x/L$ =1.0.

2.1. Equation of motion and displacement function for the beam segment

For transverse vibration of the i-th beam segment, its equation of motion is given by [22]

$$EIy_i'''' (x,t) + \rho A\ddot{y}_i(x,t) = F_i(t) \cdot \delta(x - x_{F_i})(x_{i-1} \leqslant x \leqslant x_i) \tag{1}$$

where the prime ($'$) and overhead dot ($\cdot$) respectively denote the differentiations with respect to the axial coordinate x and time t, ρ and E are respectively the mass density and Young's modulus, A and I are respectively the area and moment of inertia of the i-th beam cross-section, while $y_i(x,t)$ denotes the transverse deflection of the i-th beam segment at position x and time t. Besides, $F_i(t)$ is a force with its magnitude equal to the external load per unit length and $\delta(x - x_{F_i})$ is the Dirac delta with x_{F_i} denoting the coordinate at which the force $F_i(t)$ applies.

If $F_i(t)$ is a harmonic force and takes the form

$$F_i(t) = \bar{F}_i e^{j\omega_e t} \tag{2}$$

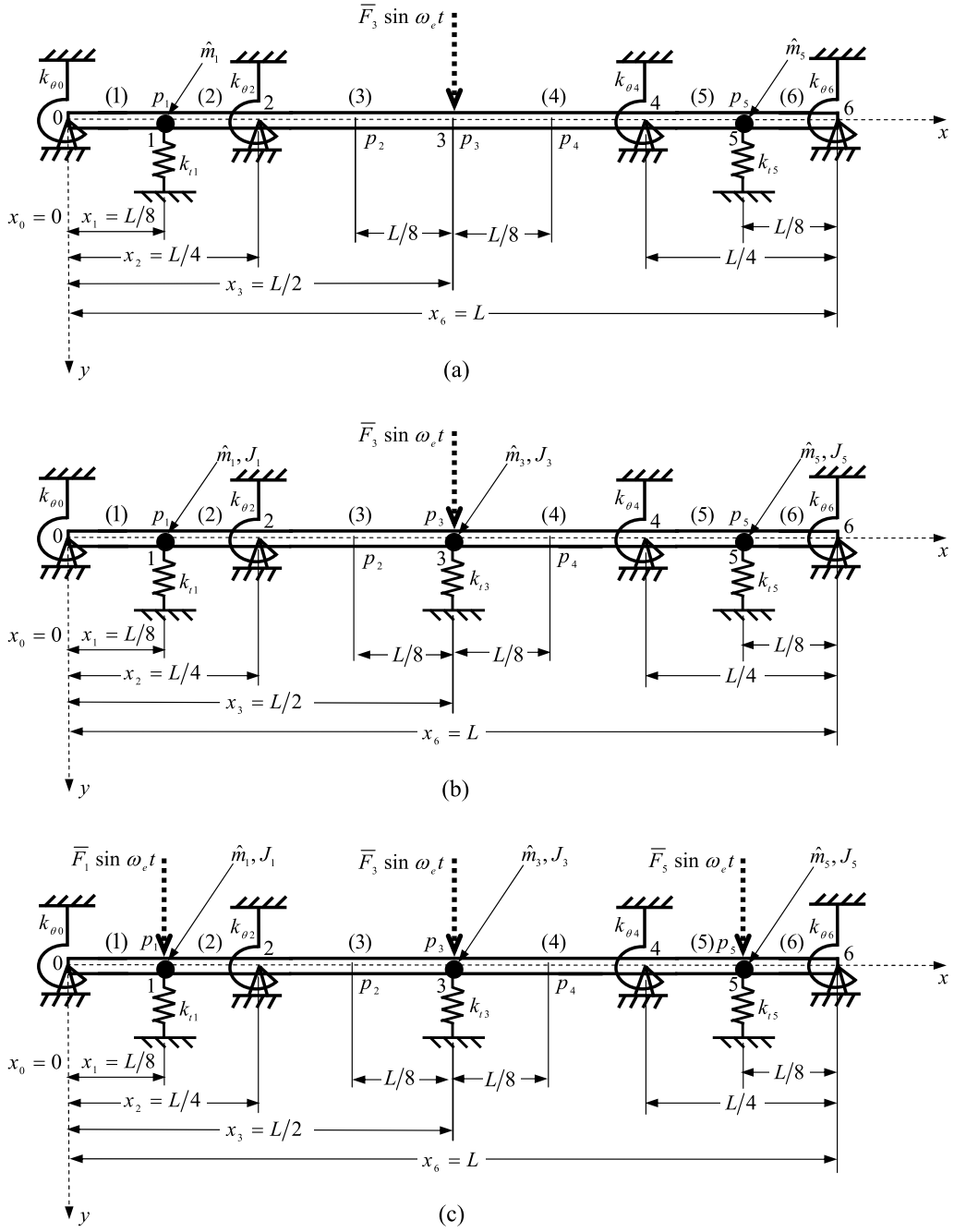

Fig. 6. A uniform beam composed of 6 uniform beam segments ((1), (2), . . . , (6)) separated by 5 nodes (1, 2, . . . , 5) and spring-hinged at node i with a rotational spring $k_{\theta\, i}$ ($i = 0$, 2, 4 and 6): (a) no concentrated elements at the position of single force $\bar{F}_3 \sin \omega_e t$ and no rotary inertia J_j ($j = 1$, 3 and 5); (b) with concentrated elements at the position of single force $\bar{F}_3 \sin \omega_e t$ and with rotary inertia J_j ($j = 1$, 3 and 5); (c) the same as (b) but having 3 forces $\bar{F}_j \sin \omega_e t$ at node j ($j = 1$, 3 and 5).

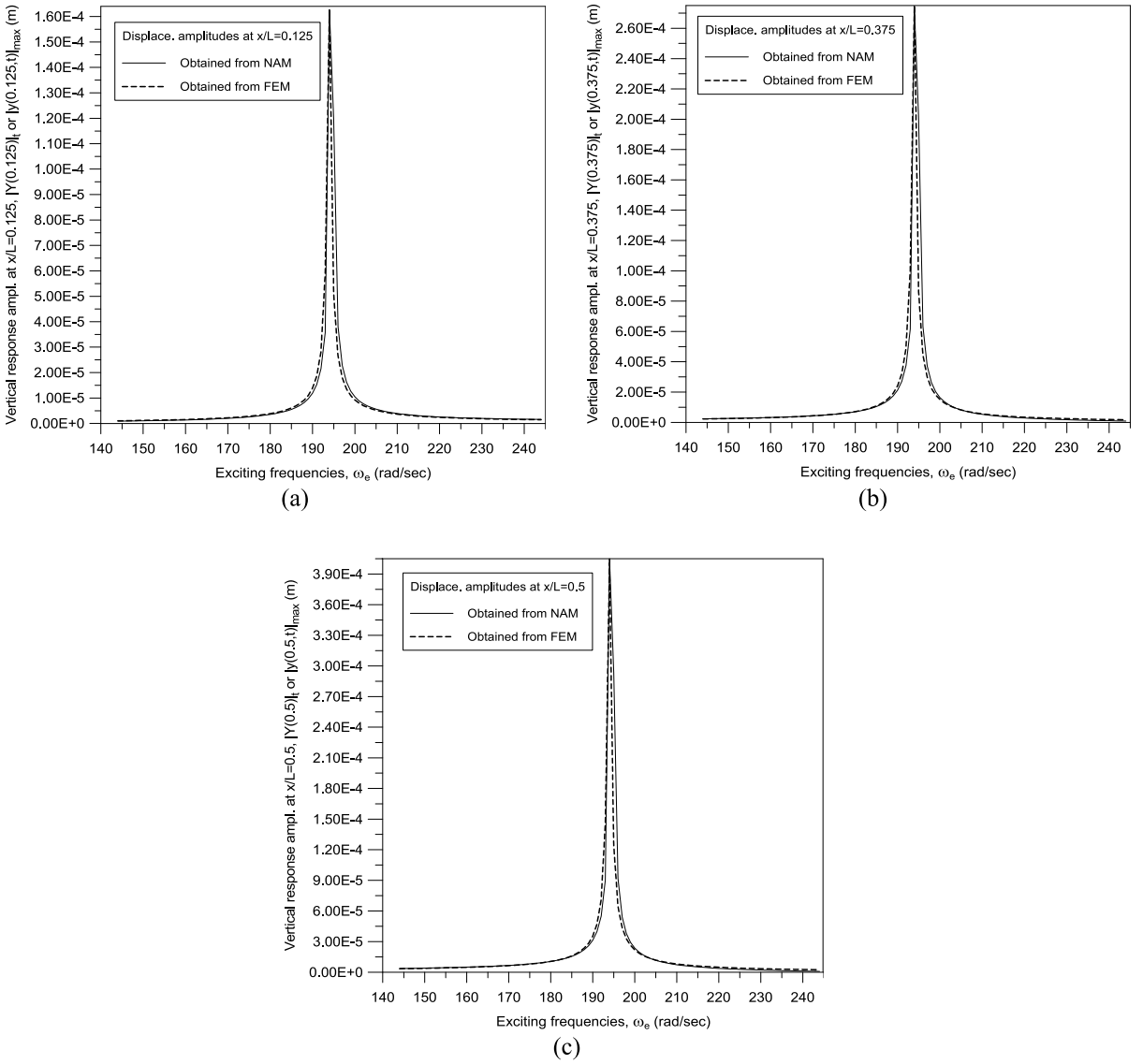

Fig. 7. The frequency-response curves for the three points p_1, p_2 and p_3 on the beam (with "zero" initial conditions) shown in Fig. 6(a), located at: (a)$\xi = x/L$ =0.125, (b)$\xi = x/L$ =0.375 and (c)$\xi = x/L$ =0.5, respectively.

then, in the steady state, one has

$$y_i(x,t) = Y_i(x)e^{j\omega_e t} \tag{3}$$

where $\bar{F}_i$ and $Y_i(x)$ are the amplitudes of $F_i(t)$ and $y_i(x,t)$, respectively, ω_e is the exciting frequency of the external load $F_i(t)$ and $j = \sqrt{-1}$.

Substituting Eqs (2) and (3) into Eq. (1), one obtains

$$Y_i''''(x) - \beta^4 Y_i(x) = \frac{\bar{F}_i}{EI}\delta(x - x_{F_i})(x_{i-1} \leqslant x \leqslant x_i) \tag{4}$$

where

$$\beta^4 = \omega_e^2 \left(\frac{\rho A}{EI}\right) \tag{5}$$

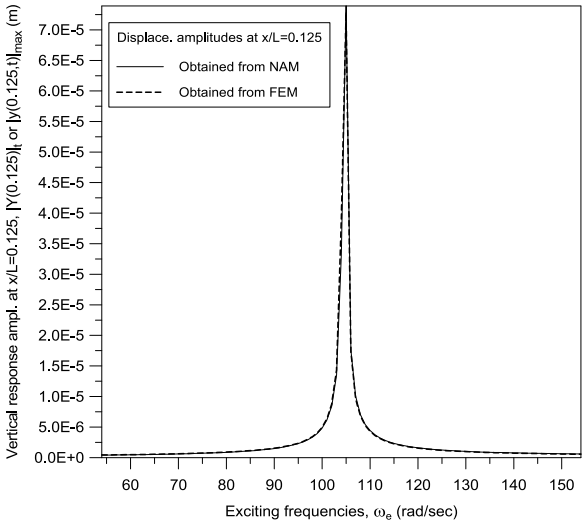

(a)

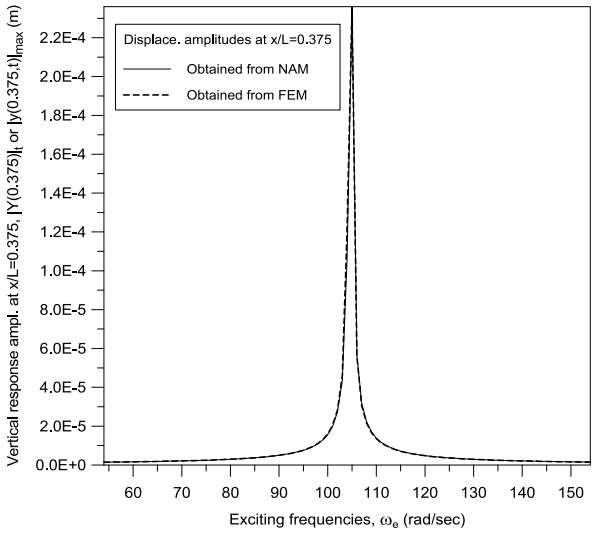

(b)

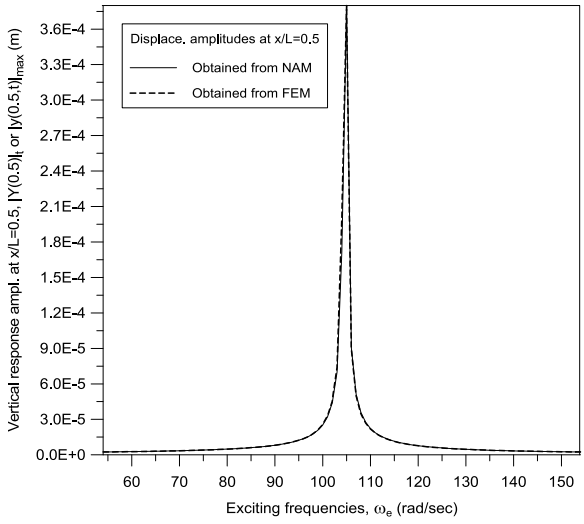

(c)

Fig. 8. The legend is the same as Fig. 7 except that this is for the vibrating system shown in Fig. 6(b).

Equation (4) is a non-homogeneous equation with x as the independent variable and its complete solution takes the form

$$Y_i(x) = \bar{A}_i \cos\beta x + \bar{B}_i \sin\beta x + \bar{C}_i \cosh\beta x + \bar{D}_i \sinh\beta x - \frac{\bar{F}_i}{\beta^4 EI}\delta(x - x_{F_i})(x_{i-1} \leqslant x \leqslant x_i) \tag{6}$$

2.2. *Compatibility of deformations and equilibrium of forces* (*and moments*) *at an intermediate node*

The continuity of displacements and slopes for the two beam segments, (i) and $(i+1)$, joined at the intermediate node i (cf. Fig. 1) requires that [22]

$$Y_i(x_i) = Y_{i+1}(x_i) \tag{7a}$$

$$Y_i'(x_i) = Y_{i+1}'(x_i) \tag{7b}$$

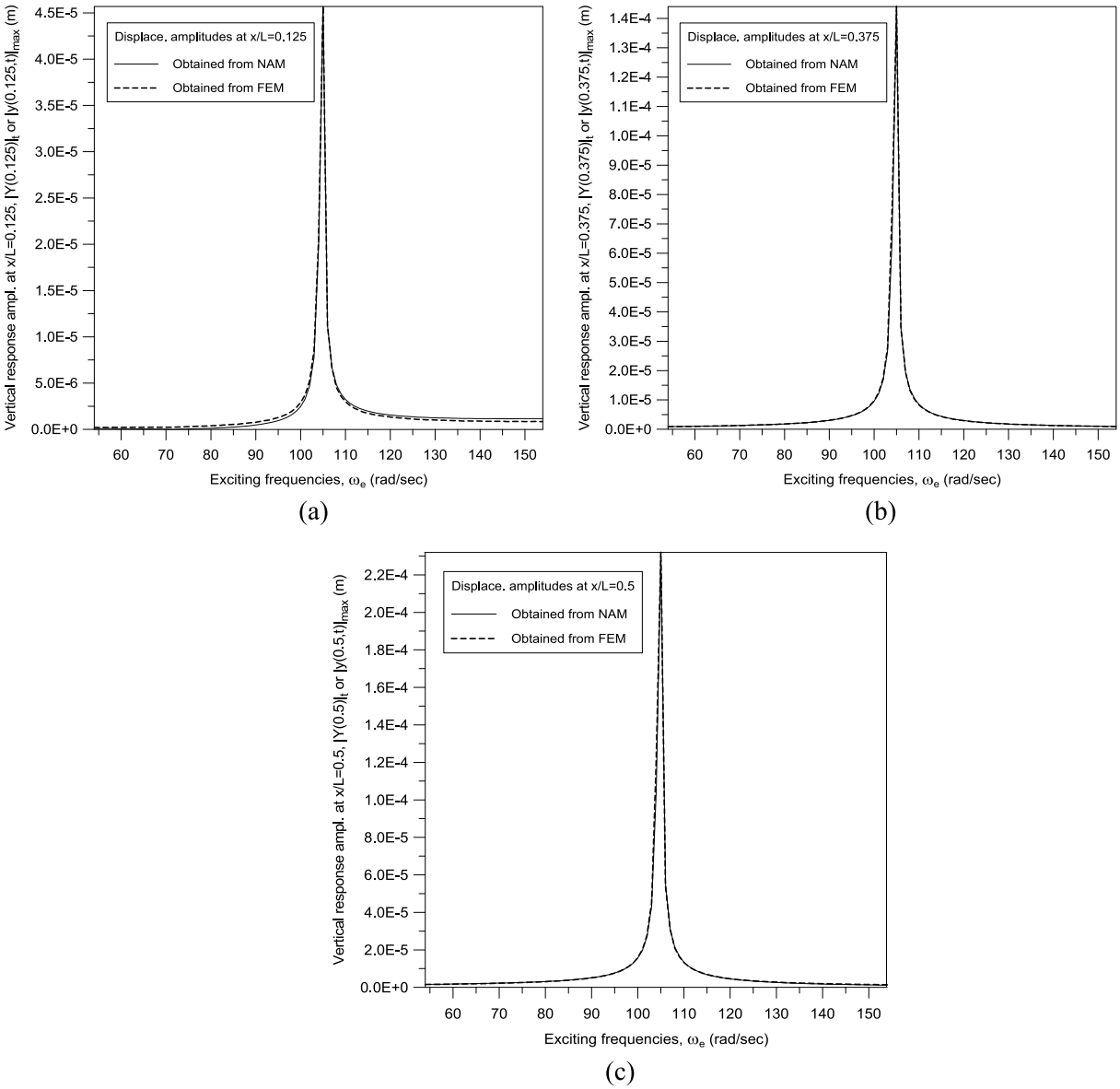

Fig. 9. The legend is the same as Fig. 7 except that this is for the vibrating system shown in Fig. 6(c).

Besides, the equilibrium of shear forces and bending moments for the last two beam segments, (i) and $(i+1)$, joined at node i requires that

$$EIY_i''(x_i) = EIY_{i+1}''(x_i) + (\omega^2 J_i - k_{\theta i})Y_i'(x_i) \tag{7c}$$

$$EIY_i'''(x_i) = EIY_{i+1}'''(x_i) - (\omega^2 \bar{m}_i - k_{ti})Y_i(x_i) - \bar{F}_i \tag{7d}$$

If $x_{F_i} = x_i$, then the substitutions of Eq. (6) into Eqs (7a)–(7d), respectively, lead to

$$\begin{aligned}&(\bar{A}_i \cos\beta x_i + \bar{B}_i \sin\beta x_i + \bar{C}_i \cosh\beta x_i + \bar{D}_i \sinh\beta x_i) - (\bar{A}_{i+1} \cos\beta x_i + \bar{B}_{i+1} \sin\beta x_i \\ &+\bar{C}_{i+1} \cosh\beta x_i + \bar{D}_{i+1} \sinh\beta x_i) = 0\end{aligned} \tag{8a}$$

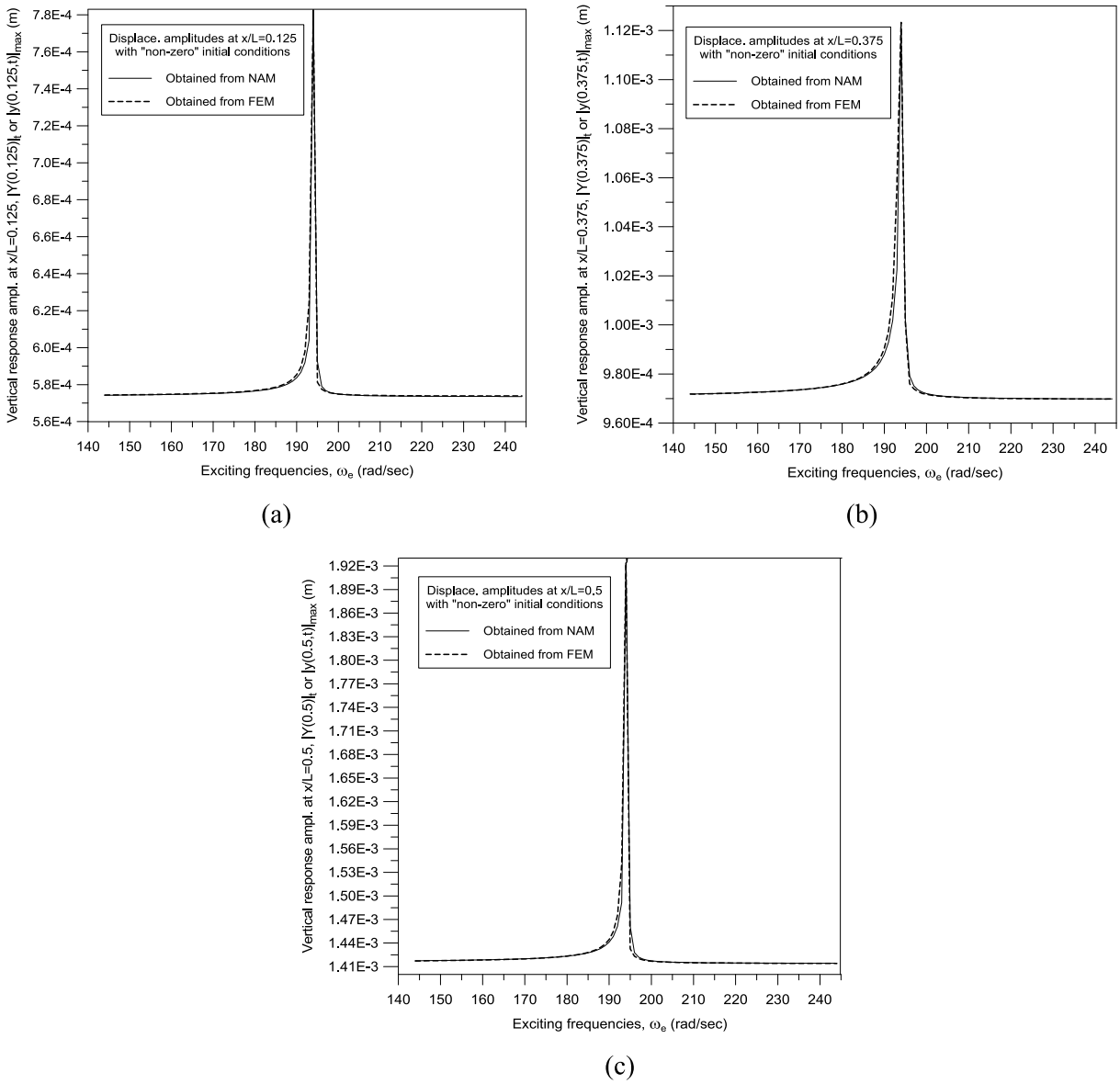

Fig. 10. The frequency-response curves for the three points p_1, p_2 and p_3 on the beam (with "non-zero" initial conditions) shown in Fig. 6(a), located at: (a)$\xi = x/L$ =0.125, (b)$\xi = x/L$ =0.375 and (c)$\xi = x/L = 0.5$, respectively.

$$
\begin{aligned}
&(-\bar{A}_i \sin\beta x_i + \bar{B}_i \cos\beta x_i + \bar{C}_i \sinh\beta x_i + \bar{D}_i \cosh\beta x_i) \\
&-(-\bar{A}_{i+1} \sin\beta x_i + \bar{B}_{i+1} \cos\beta x_i + \bar{C}_{i+1} \sinh\beta x_i + \bar{D}_{i+1} \cosh\beta x_i) = 0
\end{aligned} \tag{8b}
$$

$$
\begin{aligned}
&\bar{A}_i(\cos\beta x_i - U_i \sin\beta x_i) + \bar{B}_i(\sin\beta x_i + U_i \cos\beta x_i) \\
&+\bar{C}_i(-\cosh\beta x_i + U_i \sinh\beta x_i) + \bar{D}_i(-\sinh\beta x_i + U_i \cosh\beta x_i) \\
&-\bar{A}_{i+1} \cos\beta x_i - \bar{B}_{i+1} \sin\beta x_i + \bar{C}_{i+1} \cosh\beta x_i + \bar{D}_{i+1} \sinh\beta x_i = 0
\end{aligned} \tag{8c}
$$

$$
\begin{aligned}
&\bar{A}_i(\sin\beta x_i + R_i \cos\beta x_i) + \bar{B}_i(-\cos\beta x_i + R_i \sin\beta x_i) \\
&+\bar{C}_i(\sinh\beta x_i + R_i \cosh\beta x_i) + \bar{D}_i(\cosh\beta x_i + R_i \sinh\beta x_i) \\
&-\bar{A}_{i+1} \sin\beta x_i + \bar{B}_{i+1} \cos\beta x_i - \bar{C}_{i+1} \sinh\beta x_i - \bar{D}_{i+1} \cosh\beta x_i = -\bar{F}_i/(EI\beta^3)
\end{aligned} \tag{8d}
$$

where

$$U_i = (\omega^2 J_i - k_{\theta\, i})/(EI\beta) \tag{9a}$$

$$R_i = (\omega^2 \bar{m}_i - k_{ti})/(EI\beta^3) \tag{9b}$$

2.3. Boundary conditions for the whole vibrating system

For the "free-free" beam as shown in Fig. 1, from Eqs (7c) and (7d) one has

$$EIY_1''(x_0) + (\omega^2 J_0 - k_{\theta 0})Y_1'(x_0) = 0 \tag{10a}$$

$$-EIY_1'''(x_0) + (\omega^2 \bar{m}_0 - k_{t0})Y_1(x_0) = -\bar{F}_0 \tag{10b}$$

$$EIY_n''(x_n) - (\omega^2 J_n - k_{\theta n})Y_n'(x_n) = 0 \tag{10c}$$

$$EIY_n'''(x_n) + (\omega^2 \bar{m}_n - k_{tn})Y_n(x_n) = -\bar{F}_n \tag{10d}$$

The substitutions of Eq. (6) into Eqs (10a–d), respectively, lead to

$$\begin{aligned}&\bar{A}_1(-\cos\beta x_0 - U_0 \sin\beta x_0) + \bar{B}_1(-\sin\beta x_0 + U_0\cos\beta x_0)\\ &+\bar{C}_1(\cosh\beta x_0 + U_0\sinh\beta x_0) + \bar{D}_1(\sinh\beta x_0 + U_0\cosh\beta x_0) = 0\end{aligned} \tag{11a}$$

$$\begin{aligned}&\bar{A}_1(-\sin\beta x_0 + R_0\cos\beta x_0) + \bar{B}_1(\cos\beta x_0 + R_0\sin\beta x_0)\\ &+\bar{C}_1(-\sinh\beta x_0 + R_0\cosh\beta x_0) + \bar{D}_1(-\cosh\beta x_0 + R_0\sinh\beta x_0) = -\bar{F}_0/(EI\beta^3)\end{aligned} \tag{11b}$$

$$\begin{aligned}&\bar{A}_n(\cos\beta x_n - U_n\sin\beta x_n) + \bar{B}_n(\sin\beta x_n + U_n\cos\beta x_n)\\ &+\bar{C}_n(-\cosh\beta x_n + U_n\sinh\beta x_n) + \bar{D}_n(-\sinh\beta x_n + U_n\cosh\beta x_n) = 0\end{aligned} \tag{11c}$$

$$\begin{aligned}&\bar{A}_n(\sin\beta x_n + R_n\cos\beta x_n) + \bar{B}_n(-\cos\beta x_n + R_n\sin\beta x_n)\\ &+\bar{C}_n(\sinh\beta x_n + R_n\cosh\beta x_n) + \bar{D}_n(\cosh\beta x_n + R_n\sinh\beta x_n) = -\bar{F}_n/(EI\beta^3)\end{aligned} \tag{11d}$$

where

$$U_0 = (\omega^2 J_0 - k_{\theta 0})/(EI\beta), \quad R_0 = (\omega^2 \bar{m}_0 - k_{t0})/(EI\beta^3) \tag{12a,b}$$

$$U_n = (\omega^2 J_n - k_{\theta n})/(EI\beta), \quad R_n = (\omega^2 \bar{m}_n - k_{tn})/(EI\beta^3) \tag{13a,b}$$

2.4. Determination of "steady" response amplitudes

For a beam composed of n beam segments and separated by $n-1$ nodes as shown in Fig. 1, one may obtain four equations for each intermediate node i from Eqs (7a-d), four equations for the two ends of the entire beam from Eqs (10a-d), besides, from Eq. (6) one sees that there exist four integration constants ($\bar{A}_i$, $\bar{B}_i$, $\bar{C}_i$ and $\bar{D}_i$) for each beam segment. Therefore, for a beam composed of n beam segments and separated by $n-1$ nodes, one may obtain a set of simultaneous equations consisting of $4(n-1)+4 = 4n$ equations and $4n$ unknown integration constants. Writing the simultaneous equations in matrix form one has

$$[\mathbf{H}]_{4n\times 4n}\{\mathbf{C}\}_{4n\times 1} = \{\mathbf{f}\}_{4n\times 1} \tag{14}$$

where $\{\mathbf{C}\}$ and $\{\mathbf{f}\}$ are the $4n\times 1$ column vectors (i.e., $\{\cdots\} \equiv \{\vdots\} = [\cdots]^T$, with $\{\vdots\}$ and $[\cdots]$ denoting the *column* vector and *row* vector, respectively) to take the forms

$$\{\mathbf{C}\}_{4n\times 1} = \{\ \bar{A}_1\ \bar{B}_1\ \bar{C}_1\ \bar{D}_1\ \cdots\ \bar{A}_i\ \bar{B}_i\ \bar{C}_i\ \ \bar{D}_i\ \ \bar{A}_{i+1}\ \bar{B}_{i+1}\ \bar{C}_{i+1}\ \bar{D}_{i+1}\ \ldots\ \bar{A}_n\ \bar{B}_n\ \bar{C}_n\ \bar{D}_n\ \} \tag{15}$$

$$\{\mathbf{f}\}_{4n\times 1} = \left\{\ 0\ \tfrac{-\bar{F}_0}{EI\beta^3}\ \cdots\ 0\,0\,0\ \ \tfrac{-\bar{F}_i}{EI\beta^3}\ \ 0\,0\,0\ \tfrac{-\bar{F}_{i+1}}{EI\beta^3}\ \cdots\ 0\ \tfrac{-\bar{F}_n}{EI\beta^3}\ \right\} \tag{16}$$

and $[\mathbf{H}]$ is a $4n \times 4n$ square matrix with its "non-zero" coefficients given by (cf. Eqs (11a,b), (8a-d) and (11c,d)):

$$H_{1,1} = -\cos\beta x_0 - U_0 \sin\beta x_0, \quad H_{1,2} = -\sin\beta x_0 + U_0 \cos\beta x_0,$$
$$H_{1,3} = \cosh\beta x_0 + U_0 \sinh\beta x_0, \quad H_{1,4} = \sinh\beta x_0 + U_0 \cosh\beta x_0 \tag{17a-d}$$

$$H_{2,1} = -\sin\beta x_0 + R_0 \cos\beta x_0, \quad H_{2,2} = \cos\beta x_0 + R_0 \sin\beta x_0,$$
$$H_{2,3} = -\sinh\beta x_0 + R_0 \cosh\beta x_0, \quad H_{2,4} = -\cosh\beta x_0 + R_0 \sinh\beta x_0 \ldots \tag{18a-d}$$

$\cdots\cdots$

$$H_{4i-1,4i-3} = \cos\beta x_i, \quad H_{4i-1,4i-2} = \sin\beta x_i, \quad H_{4i-1,4i-1} = \cosh\beta x_i,$$
$$H_{4i-1,4i} = \sinh\beta x_i, \quad H_{4i-1,4i+1} = -\cos\beta x_i, \quad H_{4i-1,4i+2} = -\sin\beta x_i, \tag{19a-h}$$
$$H_{4i-1,4i+3} = -\cosh\beta x_i, \quad H_{4i-1,4i+4} = -\sinh\beta x_i$$

$$H_{4i,4i-3} = -\sin\beta x_i, \quad H_{4i,4i-2} = \cos\beta x_i, \quad H_{4i,4i-1} = \sinh\beta x_i,$$
$$H_{4i,4i} = \cosh\beta x_i, \quad H_{4i,4i+1} = \sin\beta x_i, \quad H_{4i,4i+2} = -\cos\beta x_i, \tag{20a-h}$$
$$H_{4i,4i+3} = -\sinh\beta x_i, \quad H_{4i,4i+4} = -\cosh\beta x_i$$

$$H_{4i+1,4i-3} = \cos\beta x_i - U_i \sin\beta x_i, \quad H_{4i+1,4i-2} = \sin\beta x_i + U_i \cos\beta x_i,$$
$$H_{4i+1,4i-1} = -\cosh\beta x_i + U_i \sinh\beta x_i, H_{4i+1,4i} = -\sinh\beta x_i + U_i \cosh\beta x_i, \tag{21a-h}$$
$$H_{4i+1,4i+1} = -\cos\beta x_i, H_{4i+1,4i+2} = -\sin\beta x_i \quad H_{4i+1,4i+3} = \cosh\beta x_i, H_{4i+1,4i+4} = \sinh\beta x_i$$

$$H_{4i+2,4i-3} = \sin\beta x_i + R_i \cos\beta x_i, \quad H_{4i+2,4i-2} = -\cos\beta x_i + R_i \sin\beta x_i,$$
$$H_{4i+2,4i-1} = \sinh\beta x_i + R_i \cosh\beta x_i, \quad H_{4i+2,4i} = \cosh\beta x_i + R_i \sinh\beta x_i, \tag{22a-h}$$
$$H_{4i+2,4i+1} = -\sin\beta x_i, H_{4i+2,4i+2} = \cos\beta x_i, H_{4i+2,4i+3} = -\sinh\beta x_i, H_{4i+2,4i+4} = -\cosh\beta x_i$$

$\cdots\cdots$

$$H_{4n-1,4n-3} = \cos\beta x_n - U_n \sin\beta x_n, \quad H_{4n-1,4n-2} = \sin\beta x_n + U_n \cos\beta x_n,$$
$$H_{4n-1,4n-1} = -\cosh\beta x_n + U_n \sinh\beta x_n, \quad H_{4n-1,4n} = -\sinh\beta x_n + U_n \cosh\beta x_n, \tag{23a-d}$$

$$H_{4n,4n-3} = \sin\beta x_n + R_n \cos\beta x_n, \quad H_{4n,4n-2} = -\cos\beta x_n + R_n \sin\beta x_n,$$
$$H_{4n,4n-1} = \sinh\beta x_n + R_n \cosh\beta x_n, \quad H_{4n,4n} = \cosh\beta x_n + R_n \sinh\beta x_n, \tag{24a-d}$$

For any specified exciting frequency ω_e and force amplitudes $\bar{F}_i$ (i = 0,1,2, ..., n), from Eq. (5) one may obtain the associated parameterβ and, in turn, the values of the integration constant vector $\{C\}_{4n\times 1}$ from Eq. (14), i.e.,

$$\{\mathbf{C}\}_{4n\times 1} = [\mathbf{H}]^{-1}_{4n\times 4n}\{\mathbf{f}\}_{4n\times 1} \tag{25}$$

Substituting the integration constants of each beam segment ($\bar{A}_i$, $\bar{B}_i$, $\bar{C}_i$ and $\bar{D}_i$) defined by the vector $\{\mathbf{C}\}_{4n\times 1}$ into the displacement function defined by Eq. (6) (with $\bar{F}_i = 0$), one obtains the displacement-amplitude curve for the entire system vibrating in *steady-state* condition. It is evident that one may obtain the frequency-response amplitude curve for any point of the beam by repeating the last calculating procedures with a series of exciting frequencies ω_e.

For the case of no external loads, i.e., $\bar{F}_i = 0$ (i = 0,1,2, ..., n), Eq. (14) reduces to

$$[\mathbf{H}]_{4n\times 4n}\{\mathbf{C}\}_{4n\times 1} = 0 \tag{26}$$

Which is equivalent to the equation of motion for a freely vibrating system [11–13], non-trivial solution for $\{\mathbf{C}\}_{4n\times 1}$ requires that

$$|\mathbf{H}| = 0 \tag{27}$$

The values of ω_e corresponding to the specified values of β obtained from Eq. (27) denote the natural frequencies, and the displacement amplitudes based on the integration constants $\{\mathbf{C}\}_{4n\times 1}$ obtained from Eq. (26) give the associated mode shapes of the vibrating system. The foregoing formulation is based on the numerical assembly method (NAM), for the details one may refer to reference [11].

3. Relationship between total and steady response amplitudes

In engineering, one requires the "total" response amplitude instead of the "steady" one obtained from the last section. Thus, this section aims at determining the "total" response amplitude from its "steady" component. The theory is as follows:

For a SDOF spring-mass system without damping and subjected to a harmonic force $\bar{F}\sin\omega_e t$ as shown in Fig. 2, its equation of motion is to take the form

$$m\ddot{u}(t) + ku(t) = \bar{F}\sin\omega_e t \tag{28}$$

where $\ddot{u}(t)$ is acceleration, $u(t)$ is displacement, m is lumped mass, k is stiffness coefficient, $\bar{F}$ is force amplitude, ω_e is exciting frequency and t is time.

Equation (28) is a non-homogeneous equation, its *total* (or complete) solution $u_t(t)$ is given by

$$u_t(t) = u_c(t) + u_s(t) \tag{29}$$

where $u_c(t)$ and $u_s(t)$ denote the *complementary* and *steady* (or particular) solutions of Eq. (28), respectively. They are to take the forms

$$u_c(t) = \widehat{A}\sin\omega t + \widehat{B}\cos\omega t \tag{30}$$

$$u_s(t) = \widehat{C}\sin\omega_e t \tag{31}$$

In the last two expressions, $\widehat{A}$, $\widehat{B}$ and $\widehat{C}$ are unknown constants and ω is natural frequency of the vibrating system given by

$$\omega = \sqrt{k/m} \tag{32}$$

For the case with "zero" initial displacement u_0 and "zero" initial velocity $\dot{u}_0$, i.e.,

$$u_t(0) = u_0 = 0 \ \text{ and } \ \dot{u}_t(0) = \dot{u}_0 = 0 \tag{33a,b}$$

one obtains the total solution of Eq. (28) to be

$$u_t(t) = \widehat{C}\left[-\left(\frac{\omega_e}{\omega}\right)\sin\omega t + \sin\omega_e t\right] \tag{34}$$

where

$$\widehat{C} = \frac{\bar{F}}{m(\omega^2 - \omega_e^2)} \tag{35}$$

In Eq. (34), the term consisting of "$\sin\omega t$" denotes the *complementary* solution and that consisting of "$\sin\omega_e t$" denotes the *particular* (or *steady*) solution. In other words, even if the initial conditions are "at rest", the *complementary* solution exists always and is one of the important components of the *total* (complete) solution of the vibrating system. For the equations shown in reference [22], Eq. (6a) is the "complete" solution of Eq. (4) because Eq. (4) is a function of x (in the space domain). However, in the time domain (t), Eq. (6a) is only the "steady" solution of Eq. (1) because Eq. (4) is obtained from Eq. (1) by assuming that $F(t) = \bar{F}e^{j\omega_e t}$ and $y(x,t) = Y(x)e^{j\omega_e t}$ as one may see from Eqs (2) and (3) of reference [22]. Actually, from Eq. (5a) of reference [22] one also sees that the frequency parameter β is a function of exciting frequency ω_e (rather than the natural frequency ω), thus, the solution given by Eq. (6a) or (6b) of reference [22] is only the "steady" component of the "total" solution of Eq. (1) and the "complementary" component due to free vibration with natural frequency ω is not included.

If the amplitude of *complementary* component $u_c(t)$ and that of *steady* component $u_s(t)$ are represented by $\bar{u}_c$ and $\bar{u}_s$, respectively, then from Eqs (34) and (35) one has

$$\bar{u}_c = \frac{\bar{F}\omega_e}{m\omega(\omega^2 - \omega_e^2)} \tag{36a}$$

$$\bar{u}_s = \frac{\bar{F}}{m(\omega^2 - \omega_e^2)} \tag{36b}$$

Thus, Eq. (34) may be rewritten as

$$u_t(t) = -\bar{u}_c \sin\omega t + \bar{u}_s \sin\omega_e t \tag{37}$$

From Eqs (36a,b) one obtains the amplitude ratio between $\bar{u}_c$ and $\bar{u}_s$ to be

$$\bar{u}_c/\bar{u}_s = \omega_e/\omega \tag{38}$$

From Eq. (38) one sees that $\bar{u}_c$ is less than $\bar{u}_s$ if $\omega_e < \omega$ and this trend reverses if $\omega_e > \omega$, furthermore, for the case of $\omega_e \approx \omega$ (i.e.,$\omega_e/\omega \approx 1.0$), one has

$$\bar{u}_c \approx \bar{u}_s \tag{39}$$

From Eq. (37) one finds that the phase angle $\varepsilon(t)$ between $u_c(t)$ and $u_s(t)$ changes from time to time and it is given by

$$\varepsilon(t) = (\omega_e - \omega)t \tag{40}$$

Therefore, at a certain instant, the two components ($\sin\omega t$ and $\sin\omega_e t$) in Eq. (37) will be "in phase" and the amplitude of the *total* solution will be equal to the absolute values of $\bar{u}_c$ and $\bar{u}_s$, i.e.,

$$\bar{u}_t = |\bar{u}_c| + |\bar{u}_s| \tag{41}$$

Thus, the amplitude ratio between $\bar{u}_t$ and $\bar{u}_s$ is given by

$$\frac{\bar{u}_t}{|\bar{u}_s|} = \frac{|\bar{u}_c| + |\bar{u}_s|}{|\bar{u}_s|} = 1 + \frac{|\bar{u}_c|}{|\bar{u}_s|} = 1 + \left(\frac{\omega_e}{\omega}\right) \tag{42}$$

It is seen that

$$\bar{u}_t = \left[1 + \left(\frac{\omega_e}{\omega}\right)\right] \cdot |\bar{u}_s| \tag{43}$$

The last equation reveals that one may obtain the *total* response amplitude $\bar{u}_t$ if its *steady* component $\bar{u}_s$ is given.

For the case of $\omega_e \approx \omega$ (i.e., $\omega_e/\omega \approx 1.0$), Eq. (41) or (43) reduces to

$$\bar{u}_t \approx |\bar{u}_c| + |\bar{u}_s| \approx 2|\bar{u}_s| \tag{44}$$

Since in reference [22] and most of the existing literature, the initial conditions of a vibrating system are assumed to be "at rest" (i.e, the initial displacement $u_0 = 0$ and initial velocity $\dot{u}_0 = 0$), the above formulation with "zero" initial conditions is presented for this purpose. However, it is easy to be extended to the case with "non-zero" initial conditions (i.e., $u_0 \neq 0$ and $\dot{u}_0 \neq 0$) as one may see from Appendix A at the end of this paper.

It is well known that, near resonance, the entire MDOF (or continuous) system will vibrate synchronously in a certain mode with the exciting frequency ω_e so that its dynamic behavior looks like a SDOF system. For this reason, a continuous system with infinite DOF's can be modeled by a simple SDOF system as one may see from Section 2–6 on pages 29–30 of Ref. [23]. Furthermore, based on the theory of mode-superposition method introduced in Section 13–2 on pages 193–194 of the same reference [23], a set of N (coupled) simultaneous equations of motion for a MDOF vibrating system can also be transformed into N (uncoupled) independent equations of motion by using the orthogonality conditions between the N normal mode shapes, where each of the N independent equations of motion represents a SDOF equation of motion for mode r ($r = 1 - N$). Therefore, the formulation based on the SDOF system presented in this paper can also be extended to the MDOF system as one may see from the numerical examples illustrated in the latter section.

In the existing literature, the forced vibration responses of a MDOF system are usually determined by the step-by-step numerical method [24]. In which, the "final" values of displacements $\{\mathbf{u}(t)\}_k$ and velocities $\{\dot{\mathbf{u}}(t)\}_k$ of the k-th step ($k = 1, 2, 3, \ldots$), during time $t = (k-1)\Delta t$ to $t = k\Delta t$(with Δtdenoting the step size of time), are used as the "initial" values of displacements and velocities of the (k+ 1)-th step, during time $t = k\Delta t$ to $t = (k+1)\Delta t$. Therefore, if the "initial" values of displacements and velocities for the 1st step (with $k = 1$) are called the "first-step" initial conditions and those for the other steps (with $k > 1$) are called the "intermediate-step" initial conditions, then the conventional initial conditions (u_0 and $\dot{u}_0$) given by Eqs (33a,b) for the SDOF system at time $t = 0$ are equivalent to the "first-step" initial conditions, and the responses due to the first term of Eq. (37) with natural frequency ω are equivalent to those due to the "intermediate-step" initial conditions. It is noted that, the "intermediate-step" initial values, $\{\mathbf{u}(t)\}_k$ and $\{\dot{\mathbf{u}}(t)\}_k$, are (usually) not equal to zero, even if the "first-step" initial values, $\{\mathbf{u}(0)\}_1$ and $\{\dot{\mathbf{u}}(0)\}_1$, are equal to zero. This is the reason why the first term of Eq. (37) with natural frequency ω must be considered. Furthermore, the first term of Eq. (37) cannot die out for an un-damped vibrating system.

4. Determination of total response amplitudes with FEM

In this paper, the reliability of the theory presented in the last two sections is confirmed by using the conventional finite element method (FEM) and the step-by-step numerical integration method [24]. In which, corresponding to each specified exciting frequency ω_e, the "total" response amplitude (including the "steady" component and the "complementary" one) for each point of a multi-span beam carrying various concentrated elements and subjected to external harmonic excitations (cf. Fig. 6) is obtained from the associated complete solution for the forced (transient) responses of the vibrating system. The formulation concerned is given below.

For a MDOF un-damped vibrating system, its equations of motion take the form [24]

$$[\tilde{\mathbf{M}}]\{\ddot{\tilde{\mathbf{y}}}(t)\} + [\tilde{\mathbf{K}}]\{\tilde{\mathbf{y}}(t)\} = \{\tilde{\mathbf{f}}(t)\} \tag{45}$$

where $[\tilde{\mathbf{M}}]$ and $[\tilde{\mathbf{K}}]$ are the "overall" mass matrix and stiffness matrix, respectively, while $\{\ddot{\tilde{\mathbf{y}}}(t)\}$, $\{\tilde{\mathbf{y}}(t)\}$ and $\{\tilde{\mathbf{f}}(t)\}$ are the "overall" acceleration, displacement and external loading vectors, respectively. Before imposing the boundary (constrained) conditions of the vibrating system, the order of $[\tilde{\mathbf{M}}]$ or $[\tilde{\mathbf{K}}]$ is $2(n+1) \times 2(n+1)$ and that of $\{\ddot{\tilde{\mathbf{y}}}(t)\}$, $\{\tilde{\mathbf{y}}(t)\}$ or $\{\tilde{\mathbf{f}}(t)\}$ is $2(n+1) \times 1$ with n denoting the total number of two-node beam elements. It is noted that, for a beam composed of n two-node beam elements (with $n+1$ nodes), its total degree of freedom (DOF) is $2(n+1)$, since each node has two DOF's (one for translation and one for rotation).

The *overall* mass matrix $[\tilde{\mathbf{M}}]$ and stiffness matrix $[\tilde{\mathbf{K}}]$ appearing in Eq. (45) are obtained from the *element* mass matrix **[m]** and stiffness matrix **[k]** by using the standard assembly technique of FEM. For a two-node beam *element* carrying various concentrated elements, its mass matrix **[m]** and stiffness matrix **[k]** are shown in Appendix B at the end of this paper.

For free vibrations, one has

$$\{\tilde{\mathbf{y}}(t)\} = \{\tilde{\mathbf{Y}}\}e^{j\omega t} \tag{46}$$

Substituting Eq. (46) into Eq. (45) and setting $\{\tilde{\mathbf{f}}(t)\} = 0$, one obtains the characteristic equations for free vibrations of the beam to be

$$([\tilde{\mathbf{K}}] - \omega^2[\tilde{\mathbf{M}}])\{\tilde{\mathbf{Y}}\} = 0 \tag{47}$$

In Eqs (46) and (47), the symbol $\{\tilde{\mathbf{Y}}\}$ denotes the amplitude of $\{\tilde{\mathbf{y}}(t)\}$, ω denotes the natural frequency of the vibrating system and $j = \sqrt{-1}$.

Equations (45)–(47) are for the "unconstrained" vibrating system, and the associated equations for the same system with specified boundary (constrained) conditions are given by

$$[\mathbf{M}]\{\ddot{\mathbf{y}}(t)\} + [\mathbf{K}]\{\mathbf{y}(t)\} = \{\mathbf{f}(t)\} \tag{45'}$$

$$([\mathbf{K}] - \omega^2[\mathbf{M}])\{\bar{\mathbf{Y}}\} = 0 \tag{47'}$$

where the *effective* overall mass matrix $[\mathbf{M}]$ and stiffness matrix $[\mathbf{K}]$ appearing in Eqs (45)' and (47)' are obtained from the corresponding ones, $[\tilde{\mathbf{M}}]$ and $[\tilde{\mathbf{K}}]$, appearing in Eqs (45) and (47) by eliminating the rows and columns associated with the constrained degrees of freedom. Similarly, the *effective* overall column vectors, $\{\ddot{\mathbf{y}}(t)\}$, $\{\mathbf{y}(t)\}$, $\{\mathbf{f}(t)\}$ and $\{\bar{\mathbf{Y}}\}$, appearing in Eqs (45)' and (47)' are obtained from the corresponding ones, $\{\ddot{\tilde{\mathbf{y}}}(t)\}$, $\{\tilde{\mathbf{y}}(t)\}$, $\{\tilde{\mathbf{f}}(t)\}$ and $\{\tilde{\mathbf{Y}}\}$, appearing in Eqs (45) and (47) by eliminating the rows associated with the constrained degrees of freedom.

In this paper, for free vibration analysis, the natural frequencies and mode shapes of the multi-span beam carrying various concentrated elements (cf. Fig. 6) are determined from Eq. (47)' by using the Jacobi method [24], and for forced vibration analysis, the complete solution for the transient responses of the latter beam are determined from Eq. (45)' by using the Newmark's direct integration method incorporated with the step-by-step numerical approach [24]. The "total" response amplitude $|u_t|_{\max}$, corresponding to each specified frequency ratio ω_e/ω, is obtained from the maximum absolute value of transverse displacements in the time history. For the case with non-zero initial conditions, the values of initial displacements and initial velocities are obtained from Eqs (54) and (55) in the next section.

Table 1
The lowest five natural frequencies of the cantilever beam shown in Fig. 4

Methods	Natural frequencies, ω_r (rad/sec)				
	ω_1	ω_2	ω_3	ω_4	ω_5
Present (NAM)	633.9730	3961.5442	5705.7519	12837.9421	15849.3140
[a]FEM	633.9001	3961.0957	5705.1129	12836.6122	15847.7620

[a]Total number of beam elements is $n_e = 40$.

5. Numerical results and discussions

In order to confirm the reliability of the theory presented in this paper, the frequency-response amplitude curves of a SDOF spring-mass system (cf. Fig. 2), a uniform cantilever beam with overhang (cf. Fig. 4) and a multi-span beam carrying various concentrated elements (cf. Figs 6(a)–(c)) are plotted by two methods. For convenience, the method based on Eqs (14) and (43) (or Eq. (A.6) in Appendix A) is called NAM, because the "steady" response amplitudes $|Y(x)|_s$ are obtained from the numerical assembly method (except the SDOF spring-mass system) and the other method is called FEM, because the "total" response amplitudes $|y(x,t)|_{\max}$ are obtained from *time histories* for transverse displacements of the vibrating system by using finite element method.

5.1. Frequency-response curve for a SDOF spring-mass system

For the SDOF spring-mass system shown in Fig. 2 with lumped mass $m = 1$ kg, stiffness constant $k = 10{,}000$ N/m and subjected to a harmonic force $F(t) = 1.0 \sin \omega_e t$ N, the natural frequency of the spring-mass system is $\omega = \sqrt{k/m} = \sqrt{10000/1} = 100$ rad/sec and the period is $T = 2\pi/\omega = 0.062831852$sec. Substituting the last relevant values into Eqs (36a) and (36b) one obtains

$$\bar{u}_s = \bar{F}/[m(\omega^2 - \omega_e^2)] = 1/[1 \times (10000 - \omega_e^2)] \tag{48}$$

$$\bar{u}_c = (\omega_e/\omega) \cdot \bar{F}/[m(\omega^2 - \omega_e^2)] = (\omega_e/\omega) \cdot \bar{u}_s \tag{49}$$

For the case with conventional zero initial conditions (i.e., $u_0 = \dot{u}_0 = 0$), Fig. 3(a) shows the frequency-response curves for the total amplitudes obtained from the formula $\bar{u}_t = |\bar{u}_s| + |\bar{u}_c|$(denoted by solid line ——) and the total amplitudes obtained from conventional time-history method $\bar{u}_t = |u(t)|_{\max}$ (denoted by dashed line $- - -$). In the time-history method, the time histories for the total vibration responses $u_t(t)$ of the lumped mass m due to each exciting frequency ω_e are obtained from Eq. (37) with time step $\Delta t = 0.001$ second and duration time $t_{\max} = 6$ seconds for general cases ($t_{\max} = 36$ seconds for the cases near resonance). It is evident that the solid curve (——) and the dashed curve ($- - -$) are in good agreement. Furthermore, the exciting frequency corresponding to the peak of the curve is near natural frequency of the vibrating system, i.e., $\omega_e \approx \omega = 100$ rad/sec.

If the initial conditions of the vibrating system is given by $u_0 = 0.001$ m and $\dot{u}_0 = \omega u_0 = 0.1$ m/sec, then from Eqs (A.4) and (A.5) (cf. Appendix A) one obtains

$$\bar{U}_c = \sqrt{[(-\omega_e \bar{u}_s + 0.1)/\omega]^2 + 0.001^2} \tag{50}$$

$$\theta = \tan^{-1}\{[(-\omega_e \bar{u}_s + 0.1)/\omega]/0.001\} \tag{51}$$

Based on Eqs (48), (50), (51), (A.6) and (A.3) (cf. Appendix A), and following the similar steps for the foregoing zero initial conditions (i.e., $u_0 = \dot{u}_0 = 0$), one obtains the frequency-response curves for the total response amplitudes obtained from the formula $\bar{u}_t = |\bar{u}_s| + \bar{U}_c$(denoted by ——) and the total response amplitudes obtained from conventional time-history method $\bar{u}_t = |u(t)|_{\max}$ (denoted by $- - -$) as shown in Fig. 3(b) for the "non-zero" initial conditions (i.e., $u_0 = 0.001$ m and $\dot{u}_0 = 0.1$ m/sec). It is seen that the solid curve (——) and the dashed curve ($- - -$) are in good agreement.

Table 2
The dimensionless vibration amplitudes at different positions of the cantilever beam (with "zero" initial conditions) having an intermediate pinned-support and subjected to a concentrated harmonic force at free end (cf. Fig. 4)

Locations, $\xi = x/L$	[a]Dimensionless steady amplitudes, $\lvert Y^*(\xi)\rvert_s = \lvert Y(\xi)\rvert_s / C_Y$	
	Present	Reference [22]
0.0	0.000000	0.000000
0.1	−0.001380	−0.001380
0.2	−0.004136	−0.004136
0.3	−0.006196	−0.006197
0.4	−0.005500	−0.005501
0.5	0.000000	0.000000
0.6	0.011746	0.011747
0.7	0.028811	0.028814
0.8	0.049707	0.049712
0.9	0.073017	0.073026
1.0	0.097461	0.097467

[a] $C_Y = \bar{F}L^3/(EI) = 0.15754 \times 10^{-4}$.

5.2. Frequency-response curves for a uniform cantilever beam with overhang

The vibrating system studied in this subsection (with zero initial conditions) is shown in Fig. 4. It is a cantilever beam with an intermediate pinned support at mid-length (node 1) and subjected to a harmonic concentrated force $\bar{F}_2 \sin \omega_e t$ at free end (node 2). For comparison, all given data are the same as those of reference [22]: mass density $\rho = 7836.7896$ kg/m^3, Young's modulus $E = 2.069 \times 10^{11}$ N/m^2, diameter $d = 0.05$ m, moment of inertia of cross-sectional area $I = 3.06796 \times 10^{-7}$m^4, mass per unit length $\bar{m}$ =15.3875kg/m, and total length L =1m. Comparing Fig. 4 with Fig. 1, one sees that total number of beam segments is $n = 2$ and all concentrated elements are equal to zero (i.e., $\hat{m}_i = j_i = k_{ti} = k_{\theta i} = 0$, $i = 0, 1, 2$) except that $k_{t0} = k_{t1} = 1.0 \times 10^{16} \approx \infty$ N/m and $k_{\theta 0} = 1.0 \times 10^{16} \approx \infty$ N-m/rad.

The lowest five natural frequencies of the vibrating system obtained from Eq. (26) and those obtained from the conventional FEM are shown in Table 1. It is seen that the NAM results are in good agreement with the FEM ones (with total number of beam elements $n_e = 40$). For the case of $\bar{F}_2 = 1.0$ N and $\Omega = [\omega_e^2 \bar{m} L^4/(EI)]^{1/4} = \sqrt{5}$, one has $\omega_e = \Omega^2 \sqrt{EI/(\bar{m}L^4)}$= 321.1735 rad/sec. By using Eq. (14), the dimensionless "steady" vibration amplitudes $|Y^*(\xi)|_s = |Y(\xi)|_s/C_Y$ at different positions of the cantilever beam (with $\xi = x/L = 0$, 0.1, 0.2, 0.3, ..., 0.9, 1.0) are shown in Table 2, where $C_Y = \bar{F}L^3/(EI) = 1.0 \times 1.0^3/[(2.069 \times 10^{11})(3.06796 \times 10^{-7})] = 0.15754 \times 10^{-4}$. From the table one finds that the present results are in good agreement with those of reference [22]. Because all amplitudes given by reference [22] are only the "steady" components of the "total" response amplitudes $|Y(x)|_t$, the frequency-response curves of $|Y(x)|_t$ versus ω_e are shown in Figs 5(a)–(c) for the three points p_1, p_2 and p_3 located at $\xi = x/L = 0.3$, 0.8 and 1.0, respectively. In which, the solid curves (——) denote the total response amplitudes $|Y(x)|_t$ obtained from NAM, and the short dashed curves (− − −) denote those $|y(x,t)|_{\max}$ obtained from FEM (the time-history method). Note that the time histories for the total vibration responses of the beam due to each exciting frequency ω_e are obtained with time step $\Delta t = 0.0001$ second and duration time $t_{\max} = 6$ seconds for general cases ($t_{\max} = 36$ seconds for the cases near resonance). Because of the good agreement between the solid curves (——) and short dashed curves (− − −) in Figs 5(a)–(c), the theory for the SDOF vibrating system studied in the last section can also be extended to the MDOF system studied in the current section. From Figs 5(a)–(c) one also sees that the exciting frequency corresponding to the peak of each curve is very close to the first natural frequency of the vibrating system, i.e., $\omega_e \approx \omega_1 = 633.9730$ rad/sec.

5.3. Frequency-response curves for a multi-span beam carrying various concentrated elements with "zero" initial conditions

Figures 6(a)–(c) show the three vibrating systems with "zero" initial conditions (i.e., $y_i(x,t) = 0$ and $\dot{y}_i(x,t) = 0$ at $t = 0$) studied in this subsection. They are the 3-span uniform beams with given data: mass density ρ =7850 kg/m^3,

Young's modulus $E = 2.068 \times 10^{11}$ N/m^2, diameter $d = 0.05$ m and total length $L = 4$ m. They are spring-hinged at $\xi = 0.0$, 0.25, 0.75 and 1.0, and subjected to the action of a harmonic concentrated force $\bar{F} e^{j\omega_e t}$ at $\xi = 1.0$, 0.5 or/and 0.9, respectively. The magnitude of the applied force is $\bar{F}_i = 1.0$ N. The main differences between the three vibrating systems are: In Fig. 6(a), the rotary inertias of all lumped masses are equal to zero (i.e., $J_i = 0$, i = 1,3,5), besides, all external forces are equal to zero except the one applied at node 3 (i.e., $\bar{F}_3 \sin\omega_e t$) and there exists no concentrated elements at node 3 (i.e., $m_3 = J_3 = k_{t3} = k_{\theta 3} = 0$). In Fig. 6(b), all conditions are the same as Fig. 6(a) except that the rotary inertias of all lumped masses are considered (i.e., $J_i \neq 0$, i = 1,3,5), besides, there exist one set of concentrated elements (including m_3, J_3 and k_{t3}) at the applied point (i.e., node 3) of the single external force $\bar{F}_3 \sin\omega_e t$. In Fig. 6(c), all conditions are the same as Fig. 6(b) except that two additional external forces ($\bar{F}_1 \sin\omega_e t$ and $\bar{F}_5 \sin\omega_e t$) are applied on nodes 1 and 5, respectively.

Comparing Figs 6(a)–(c) with Fig. 1 one sees that, for the current vibrating systems, the total number of beam segments is $n = 6$ (denoted by (1), (2), ..., (6)) and total number of nodes is 7 (denoted by 0, 1, 2, ..., 5, 6). For convenience, the following parameters are introduced: reference mass $\tilde{m} = \rho AL$ =61.653753 kg, reference rotary inertia $\tilde{J} = \rho AL^3$ =986.459888 kg-m^2, reference translational spring constant $\tilde{k}_t = EI/L^3$ =991.33505968 N/m, reference rotational spring constant $\tilde{k}_\theta = EI/L$ =15861.360955 N-m/rad, with $A = \pi d^2/4 = 19.63495 \times 10^{-4}$m^2 and $I = \pi d^4/64 = 30.679615 \times 10^{-8}$m^4. Besides, it is assumed that $k_{ti} = 10^{16} \approx \infty$ N/m (for the pinned supports) and the magnitudes of the "non-zero" concentrated elements are: $\hat{m}_i = \tilde{m}$ =61.653753 kg, $J_i = 0.01\tilde{J} = 9.86460$ kg-m^2, $k_{ti} = 0.1\tilde{k}_t = 99.133506$ N/m, and $k_{\theta i} = 0.1\tilde{k}_\theta = 1586.13606$ N-m/rad. The lowest five natural frequencies of the three vibrating systems as shown in Fig. 6(a)–(c) are listed in Table 3. It is seen that the lowest five natural frequencies of Fig. 6(a) are much higher than those of Fig. 6(b) or 6(c), this is because all concentrated elements are removed from center of the beam (at node 3) and the rotary inertias of the lumped mass are also neglected in Fig. 6(a). Besides, the lowest five natural frequencies obtained from NAM are very closed to those obtained from FEM (with total number of beam elements $n_e = 80$).

For the vibrating system shown in Fig. 6(a) subjected to a central vertical force $\bar{F}_3 \sin\omega_e t$ (applied at node 3) with $\bar{F}_3 = 1.0$ N, the frequency-response curves of the three points p_1, p_2 and p_3 on the beams located at $\xi = x/L =$ 0.125, 0.375 and 0.5 are shown in Figs 7(a)–(c), respectively. Because the structural system and the external load are symmetric with respect to the vertical line passing through beam center (at node 3), the frequency-response curves of the other two points p_4 and p_5 on the beams located at $\xi = x/L = 0.625$ and 0.875 are exactly the same as those of the two points p_2 and p_1 located at $\xi = x/L = 0.375$ and 0.125, respectively, and are neglected in this paper. In Figs 7(a)–(c), the solid curves (——) are obtained from NAM (cf. Eqs (14)–(25)) and the relationship $|Y(x)|_t = [1 + (\omega_e/\omega_1)] \cdot |Y(x)|_s$, while the dashed curves (– – –) are obtained from time history method by using FEM (with time step $\Delta t = 0.001$ sec, $t_{\max} = 6$ seconds for general cases and $t_{\max} = 36$ seconds for the cases near resonance). It is seen that the solid curves (——) are very close to the dashed curves (– – –), besides, the exciting frequency corresponding to the peak of each curve is very close the first natural frequency (i.e., $\omega_e \approx \omega_1 = 194.5373$ rad/sec), thus the presented approach can also be extended to the title problem. Since the CPU time required by NAM is about 2 seconds (for IBM PC Pentium III) and that required by FEM is more than 1 hour (3600 seconds), the efficiency of the presented approach is much higher than that of the conventional time-history method (FEM).

The last conclusions obtained from the frequency-response curves of Figs 7(a)–(c) are also suitable for those shown in Figs 8(a)–(c) (for the vibrating system of Fig. 6(b)) and in Figs 9(a)–(c) (for the vibrating system of Fig. 6(c)), respectively. In addition to the resonant frequencies, the other main difference between Figs 7, 8 and 9 is the magnitudes of response amplitudes. From last three figures, one sees that the response amplitudes shown in Fig. 9 (for the vibrating system of Fig. 6(c)) are smaller than those shown in Fig. 7 (for the vibrating system of Fig. 6(a)) or Fig. 8 (for the vibrating system of Fig. 6(b)), this is due to the fact that the responses of the structural system (cf. Fig. 6(c)) induced by $\bar{F}_3 \sin\omega_e t$ (applied at node 3) are opposite to those induced by both $\bar{F}_1 \sin\omega_e t$ (applied at node 1) and $\bar{F}_5 \sin\omega_e t$ (applied at node 5). In addition, one of the major differences between Figs 6(a) and (b) is that there exists a translational spring k_{t3} located at the applied point (node 3) of the single force $\bar{F}_3 \sin\omega_e t$ in Fig. 6(b) and this should be one of the reasons why the response amplitudes shown in Fig. 8 (for the vibrating system of Fig. 6(b)) are smaller than those shown in Fig. 7 (for the vibrating system of Fig. 6(a)).

Table 3
The lowest five natural frequencies of the three vibrating systems shown in Figs 6(a)–(c), respectively

Vibrating systems	Methods	Natural frequencies, ω_r (rad/sec)				
		ω_1	ω_2	ω_3	ω_4	ω_5
Fig. 6(a)	Present (NAM)	194.5373	246.1372	340.3893	833.9799	1636.7596
	[a]FEM	194.5373	246.1372	340.3893	833.9808	1636.2302
Figs 6(b) and 6(c)	Present (NAM)	104.6888	195.6329	252.6310	255.5445	297.3698
	[a]FEM	104.6888	195.6329	252.6310	255.5445	297.3698

[a]Total number of beam elements is $n_e = 80$.

5.4. *Frequency-response curves for a multi-span beam carrying various concentrated elements with "non-zero" initial conditions*

The purpose of this subsection is to show the availability of the presented theory for the case with "non-zero" initial conditions. The structural system is the same as Fig. 6(a) studied in the last subsection except that, instead of "at rest", the initial displacements and velocities of the beam are given by $y(x,0) = 0.001\bar{Y}_1(x)$m and $\dot{y}(x,0) = \omega_1 y(x,0) = 0.001\omega_1\bar{Y}_1(x)$m/sec, respectively. Where ω_1 (=194.5373 rad/sec) is the 1st natural frequency of the beam and $\bar{Y}_1(x)$ is the corresponding 1st normal mode shape (with maximum mode displacement being equal to 1.0). From the last subsection one obtains the 1st normal mode shape of the beam shown in Fig. 6(a) to be

$$\{\bar{\mathbf{Y}}(x)\}_1 = [\ldots \bar{Y}_1(0.5)\ldots \bar{Y}_1(1.5)\ldots \bar{Y}_1(2.0)\ldots]^T = [\ldots 0.4055\ldots\text{-}0.6858\ldots -1.0\ldots]^T \tag{52}$$

Thus, the initial displacements$\{\mathbf{y}(0)\}$and initial velocities $\{\dot{\mathbf{y}}(0)\}$of the beam are given by

$$\{\mathbf{y}(0)\} = 0.001\{\bar{\mathbf{Y}}(x)\}_1 = 10^{-4}[\ldots 4.055\ldots -6.858\ldots -10.0\ldots]^T\text{m} \tag{53a}$$

$$\{\dot{\mathbf{y}}(0)\} = 0.001\omega_1\{\bar{\mathbf{Y}}(x)\}_1 = 10^{-2}[\ldots 7.888\ldots -13.341\ldots -19.454\ldots]^T\text{ m/sec} \tag{53b}$$

In the above equations, the symbols $\{\}$ and [] represent the column and row vectors, respectively. In Eq. (53a), the coefficients of the vector $\{\mathbf{y}(0)\}$ include the initial displacements of various points along the beam length, while in Eq. (53b), the coefficients of the vector $\{\dot{\mathbf{y}}(0)\}$ include the initial velocities of the corresponding points. For the NAM, only the initial displacements and initial velocities located at p_1 (at $x = 0.5$ m), p_2 (at $x = 1.5$ m) and p_3 (at $x =$ 2.0 m) are required, because only the frequency-response curves for points p_1, p_2 and p_3 are studied here. However, for the FEM, the entire beam is composed of 80 identical beam elements (i.e., $n_e = 80$) and 81 nodes with length of each beam element being $\Delta\ell = L/n_e = 4/80 = 0.05$m. Since each node has two DOF's (one for translation and one for rotation), the entire vibrating system has 162 DOF's. Therefore, the 1st normal mode shape$\{\bar{\mathbf{Y}}\}_{1,FEM}$, the initial-displacement vector $\{\mathbf{y}(0)\}$ and the initial-velocity vector $\{\dot{\mathbf{y}}(0)\}$ are the 162×1 column vectors, before imposing the boundary (constrained) conditions. Where the 1st normal mode shape $\{\bar{\mathbf{Y}}\}_{1,FEM}$ of the beam is obtained from the FEM and is to take the form

$$\{\bar{\mathbf{Y}}(x)\}_1 = \{\bar{\mathbf{Y}}\}_{1,FEM} = [\,\bar{Y}_1\ \bar{Y}_1'\ \cdots \bar{Y}_{41}\ \bar{Y}_{41}'\ \cdots \bar{Y}_{81}\ \bar{Y}_{81}'\,]^T (with \bar{Y}_{41} = 1.0) \tag{54}$$

In such a situation, the initial displacements $\{\mathbf{y}(0)\}$ and initial velocities $\{\dot{\mathbf{y}}(0)\}$ of the beam for FEM are given by

$$\{\mathbf{y}(0)\} = 0.001(\bar{\mathbf{Y}}\}_{1,FEM} = 0.001[\,\bar{Y}_1\ \bar{Y}_1'\ \cdots \bar{Y}_{41}\ \bar{Y}_{41}'\ \cdots \bar{Y}_{81}\ \bar{Y}_{81}'\,]\text{ m} \tag{55a}$$

$$\{\dot{\mathbf{y}}(0)\} = 0.001\omega_1(\bar{\mathbf{Y}}\}_{1,FEM} = 0.001\omega_1[\,\bar{Y}_1\ \bar{Y}_1'\ \cdots \bar{Y}_{41}\ \bar{Y}_{41}'\ \cdots \bar{Y}_{81}\ \bar{Y}_{81}'\,]\text{ m/sec} \tag{55b}$$

In Eqs (54) and (55a,b), $\bar{Y}_j$ and $\bar{Y}_j'$ denote the translational and rotational mode displacements of node j ($j = 1, 2, \ldots, 41, \ldots, 81$), respectively. In other words, the coefficients of the vectors $\{\mathbf{y}(0)\}$ and $\{\dot{\mathbf{y}}(0)\}$ respectively include 162 initial displacements and 162 initial velocities of the points located at $x_j = (j-1)\Delta\ell$ and are determined by Eqs (55a,b).

From Eqs (53a,b) one sees that the initial displacements and initial velocities of points p_1, p_2 and p_3 are given by ($u_{0,p_1} = 4.055 \times 10^{-4}$ m, $\dot{u}_{0,p_1} = 7.888 \times 10^{-2}$m/s), ($u_{0,p_2} = -6.858 \times 10^{-4}$ m, $\dot{u}_{0,p_2} = -13.341 \times 10^{-2}$ m/s) and ($u_{0,p_3} = -10.0 \times 10^{-4}$ m, $\dot{u}_{0,p_3} = -19.454 \times 10^{-2}$m/s), respectively, and from the last subsection (for zero initial conditions) one has obtained the "steady" components of the total response amplitudes ($\bar{u}_{s,p_1}$, $\bar{u}_{s,p_2}$ and $\bar{u}_{s,p_3}$) of points p_1, p_2 and p_3 corresponding to the exciting frequencies $\omega_e = 144$ to 244 rad/sec. Therefore, by using Eqs (A.4)

and (A.6) (cf. Appendix A), one obtains the frequency-response curves for points p_1, p_2 and p_3, with "non-zero" initial conditions, as shown in Figs 10(a), (b) and (c), and denoted by the solid lines (——), respectively. Instead of the conventional "zero" initial conditions, if the "first-step" initial conditions in the last subsection are replaced by the "non-zero" ones given by Eqs (55a,b), the frequency-response curves for points p_1, p_2 and p_3 obtained from the time-history method by using the FEM are also shown in Figs 10(a), (b) and (c), and denoted by the dashed lines (– – –), respectively. Good agreements between the solid lines and the corresponding dashed lines in Figs 10(a), (b) and (c) confirm the reliability of the presented theory for the case with "non-zero" initial conditions.

6. Conclusions

1. For the structural design, the forced vibration amplitude of a vibrating system near first natural (resonant) frequency ω_1 is one of the important information. Based on the relationship $|Y(x)|_t = [1 + (\omega_e/\omega_1)] \cdot |Y(x)|_s$, with $|Y(x)|_t$ and $|Y(x)|_s$ respectively denoting the *total* and *steady* response amplitudes at position x and ω_e denoting the exciting frequency, one may easily determine the forced vibration response amplitudes of a multi-span beam carrying arbitrary concentrated elements by using NAM with the CPU time to be much less than that required by using FEM. It is noted that $|Y(x)|_t \approx 2|Y(x)|_s$ if $\omega_e \approx \omega_1$. The above conclusion is for the conventional case with "zero" initial conditions, for the case with "non-zero" initial conditions one may refer to the Appendix A at the end of this paper. Furthermore, it can also be extended to the higher vibration modes such as $\omega_e \approx \omega_3$ and $\omega_e \approx \omega_4$ shown in Fig. A.2 of Appendix C (with "zero" initial conditions), where the solid lines (—) denote the frequency-response curve of point p_1 on the beam shown in Fig. 6(c) near $\omega_3 =$ 252.6310 rad/sec obtained from NAM, the dashed lines $(- - -)$ denote that near $\omega_4 =$ 255.5445 rad/sec $\approx \omega_3$ obtained from NAM and the dash-dot lines $(- \cdot -)$ denote that in the range of exciting frequencies $\omega_e = 230 \sim 275$ rad/sec obtained from the conventional FEM. Because $\omega_3 \approx \omega_4$, the solid lines are vary close to the dashed lines and both of them are very close to the dash-dot lines.
2. In general, checking the numerical values of forced vibration response amplitudes of a multi-degree-of-freedom (MDOF) structural system is not easy, from the foregoing numerical results and discussions one sees that the presented approach will be significant for this matter.
3. The presented approach is suitable for the general vibrating systems. For example, the beam may be single or multiple spans and with or without carrying various concentrated elements; the external force may be single or multiple and with or without various concentrated elements attached to each of the applied points, and the initial conditions may be "zero" or "non-zero".
4. In theory, the presented approach can be extended to the determination of frequency-response curves of multi-step beams or framed structures.

Acknowledgement

The financial support of National Science Council of ROC (NSC97-2611-E-006-021) is much appreciated.

Appendix A

Response amplitude for the case with "non-zero" initial conditions

For a SDOF system, its response due to initial displacement u_0 and initial velocity $\dot{u}_0$ is given by [23]

$$u(t) = u_0 \cos \omega t + (\dot{u}_0/\omega) \sin \omega t \tag{A.1}$$

From Eqs (A.1) and (37), one obtains the total response of the SDOF system at time t is given by

$$u_t(t) = [-\bar{u}_c + (\dot{u}_0/\omega)] \sin \omega t + u_0 \cos \omega t + \bar{u}_s \sin \omega_e t \tag{A.2}$$

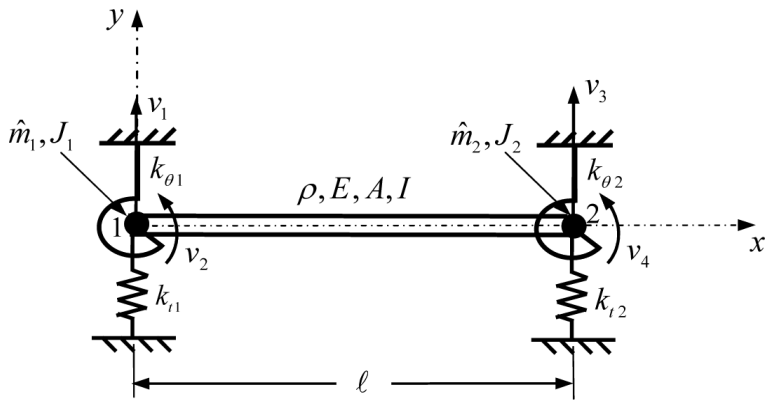

Fig. A.1. A two-node beam element carries a linear spring k_{ti}, a rotational spring $k_{\theta i}$, and a lumped mass $\hat{m}_i$ with rotary inertia J_i at each node i ($i = 1,2$) and has four degrees of freedom (DOF's), v_1, v_2, v_3 and v_4, where v_1 and v_3 are the translational DOF's and v_2 and v_4 are the rotational DOF's.

or

$$u_t(t) = \bar{U}_c \cos(\omega t - \theta) + \bar{u}_s \sin \omega_e t \tag{A.3}$$

where

$$\bar{U}_c = \sqrt{[(-\omega_e \bar{u}_s + \dot{u}_0)/\omega]^2 + u_0^2} \tag{A.4}$$

$$\theta = \tan^{-1}\{[(-\omega_e \bar{u}_s + \dot{u}_0)/\omega]/u_0\} \tag{A.5}$$

Based on Eq. (A.3), one obtains the total response amplitude of the SDOF system to be

$$\bar{u}_t = \bar{U}_c + |\bar{u}_s| \tag{A.6}$$

Equation (A.4) indicates that, for a SDOF system with natural frequency ω, one may obtain the value of $\bar{U}_c$ if the "steady" component $\bar{u}_s$ (corresponding to the exciting frequency ω_e) and the initial conditions (u_0 and $\dot{u}_0$) are given. Finally, the total response amplitude $\bar{u}_t$ is determined by Eq. (A.6).

Appendix B

Property matrices for a two-node beam element carrying various concentrated elements

For a two-node beam element carrying a linear spring k_{ti}, a rotational spring $k_{\theta i}$, a lumped mass $\hat{m}_i$ with rotary inertia J_i at each node i ($i = 1,2$) as shown in Fig. A.1, its mass matrix [**m**] and stiffness matrix [**k**] are given by [23, 24]

$$[\mathbf{m}] = \frac{\rho A \ell}{420} \begin{bmatrix} 156 + \hat{m}_1 & 22\ell & 54 & -13\ell \\ 22\ell & 4\ell^2 + J_1 & 13\ell & -3\ell^2 \\ 54 & 13\ell & 156 + \hat{m}_2 & -22\ell \\ -13\ell & -3\ell^2 & -22\ell & 4\ell^2 + J_2 \end{bmatrix} \tag{A.7}$$

$$[\mathbf{k}] = \begin{bmatrix} (12EI/\ell^3) + k_{t1} & 6EI/\ell^2 & -12EI/\ell^3 & 6EI/\ell^2 \\ 6EI/\ell^2 & (4EI/\ell) + k_{\theta 1} & -6EI/\ell^2 & 2EI/\ell \\ -12EI/\ell^3 & -6EI/\ell^2 & (12EI/\ell^3) + k_{t2} & -6EI/\ell^2 \\ 6EI/\ell^2 & 2EI/\ell & -6EI/\ell^2 & (4EI/\ell) + k_{\theta 2} \end{bmatrix} \tag{A.8}$$

where ρ and E are mass density and Young's modulus of the beam material, respectively, A is cross-sectional area of the beam, I is moment of inertia of the cross-sectional area A and ℓ is length of the beam element. It is noted that, in Refs [23,24], only the mass matrix [**m**] and stiffness matrix [**k**] of the two-node beam element *without* any attachments are given.

Appendix C

Frequency-response curves near 3rd and 4th natural frequencies for point p_1 in Fig. 6(c) obtained from NAM and FEM

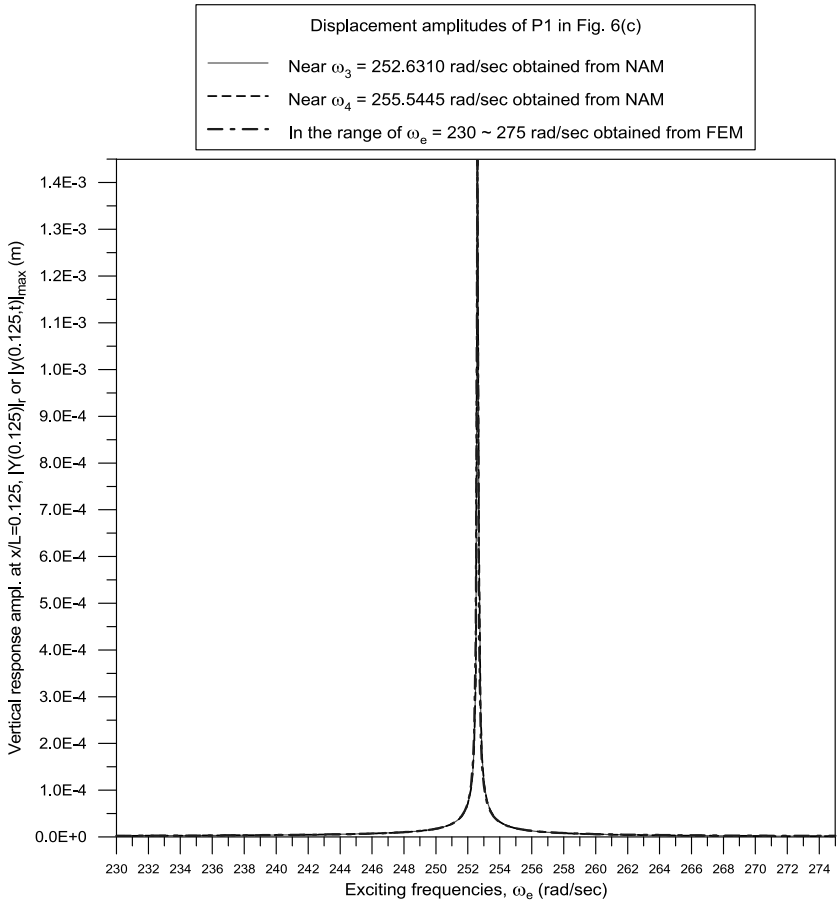

Fig. A.2. The frequency-response curves of point p_1 located at $\xi = x/L = 0.125$ on the beam shown in Fig. 6(c) (with "zero" initial conditions) near $\omega_3 = 252.6310$ rad/sec obtained from NAM (denoted by —), near $\omega_4 = 255.5445$ rad/sec obtained from NAM (denoted by $- - -$) and in the range of exciting frequencies $\omega_e = 230 \sim 275$ rad/sec obtained from FEM (denoted by $- \cdot -$), respectively.

References

[1] M.J. Maurizi, R.E. Rossi and J.A. Reyes, Vibration frequencies for a uniform beam with one end spring-hinged and subjected to a translational restraint at the other end, *Journal of Sound and Vibration* **48**(4) (1976), 565–568.
[2] A. Rutenberg, Vibration frequencies for a uniform cantilever with a rotational constraint at a point, Transactions of the ASME, *Journal of Applied Mechanics* **45** (1978), 422–423.
[3] K. Takahashi, Eigenvalue problem of a beam with a mass and spring at the end subjected to an axial force, *Journal of Sound and Vibration* **71**(3) (1980), 453–457.
[4] N.G. Stephen, Vibration of a cantilevered beam carrying a tip heavy body by Dunkerley's method, *Journal of Sound and Vibration* **70**(2) (1980), 463–465.
[5] J.H. Lau, Vibration frequencies and mode shapes for a constrained cantilever, Transactions of the ASME, *Journal of Applied Mechanics* **51** (1984), 182–187.
[6] M. Gurgoze, A note on the vibrations of restrained beams and rods with point masses, *Journal of Sound and Vibration* **96**(4) (1984), 461–468.
[7] M. Gurgoze, On the vibrations of restrained beams and rods with heavy masses, *Journal of Sound and Vibration* **100**(4) (1985), 588–589.

[8] W.H. Liu and C.C. Huang, Vibrations of a constrained beam carrying a heavy tip body, *Journal of Sound and Vibration* **123**(1) (1988), 15–29.
[9] J.S. Wu and T.L. Lin, Free vibration analysis of a uniform beam with point masses by an analytical-and-numerical-combined method, *Journal of Sound and Vibration* **136**(2) (1990), 201–213.
[10] J.S. Wu and H.M. Chou, Free vibration analysis of a cantilever beam carrying any number of elastically mounted point masses with the analytical-and-numerical- combined method, *Journal of Sound and Vibration* **213** (1998), 317–332.
[11] J.S. Wu and H.M. Chou, A new approach for determining the natural frequencies and mode shapes of a uniform beam carrying any number of sprung masses, *Journal of Sound and Vibration* **220** (1999), 451–468.
[12] D.W. Chen, The exact solutions for the natural frequencies and mode shapes of non-uniform beams carrying multiple various concentrated elements, *Structural Engineering and Mechanics* **16**(2) (2003), 153–176.
[13] H.Y. Lin and Y.C. Tsai, Free vibration analysis of a uniform multi-span beam carrying multiple spring-mass systems, *Journal of Sound and Vibration* **302** (2007), 442–456.
[14] A.C. Lee, Y. Kang and S.L. Liu, A modified transfer matrix for linear rotor-bearing systems, *Trans ASME*, *Journal of Applied Mechanics* **58** (1991), 776–783.
[15] R. Firoozian and H. Zhu, A hybrid method for the vibration analysis of rotor-bearing systems, *Proceedings of the Institute of Mechanical Engineers, part C* **205** (1991), 131–137.
[16] M. Aleyaasin, M. Ebrahimi and R. Whalley, Multivariable hybrid models for rotor-bearing systems, *Journal of Sound and Vibration* **233** (2000), 835–856.
[17] M. Aleyaasin, M. Ebrahimi and R. Whalley, Vibration analysis of distributed-lumped rotor systems, *Computer Methods in Applied Mechanics and Engineering* **189** (2000), 545–558.
[18] P.L.Verniere De Irassar, G.M. Ficcadenti and P.A.A. Laura, Dynamic analysis of a beam with an intermediate elastic support, *Journal of Sound and Vibration* **96** (1984), 381-389.
[19] M.N. Hamdan and B.A. Jubran, Free and forced vibrations of a restrained uniform beam carrying an intermediate lumped mass and a rotary inertia, *Journal of Sound and Vibration* **150** (1991), 203–216.
[20] O.S. Sener and H.N. Ozguven, Dynamic analysis of geared shaft systems by using a continuous system model, *Journal of Sound and Vibration* **166**(3) (1993), 539–556.
[21] M. Abu-Hilal, Forced vibration of Euler-Bernoulli beams by means of dynamic Green functions, *Journal of Sound and Vibration* **267** (2003), 191–207.
[22] H.Y. Lin, Dynamic analysis of a multi-span uniform beam carrying a number of various concentrated elements, *Journal of Sound and Vibration* **309** (2008), 262–275.
[23] R.W. Clough and J. Penzien, *Dynamics of Structures*, McGraw-Hill, New York, 1975.
[24] K.J. Bathe, *Finite Element Procedures in Engineering Analysis*, Prentice-Hall International, New York, 1982.
[25] L. Meirovitch, *Analytical Methods in Vibrations*, Macmillan, London, 1967.

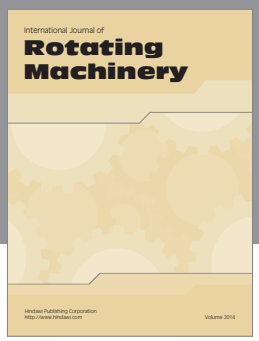

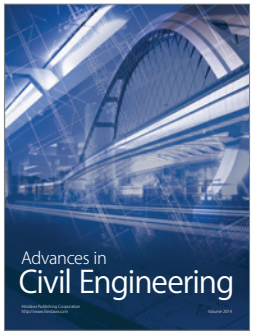

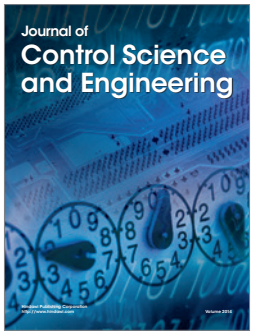

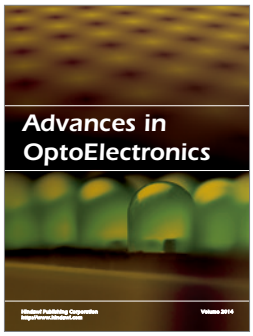

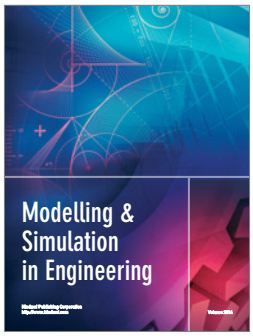

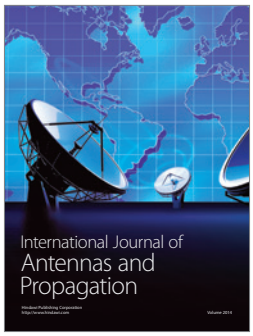

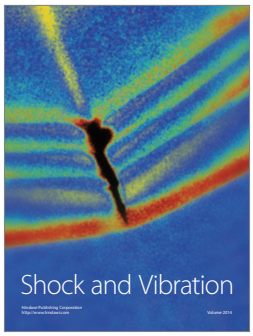

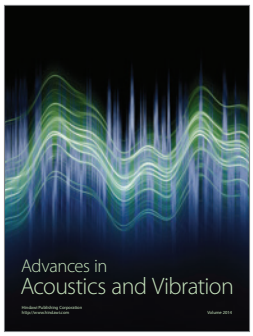

Hindawi

Submit your manuscripts at
http://www.hindawi.com